FRAME WAVELETS IN HIGH DIMENSION

by

Wei HUANG

A dissertation submitted to the faculty of
The University of North Carolina at Charlotte
in partial fulfillment of the requirements
for the degree of Doctor of Philosophy in
Mathematics

Charlotte

2016

Approved by:

Dr. Xingde DAI

Dr. Yuanan DIAO

Dr. Evan G. HOUSTON

Dr. Wei ZHAO

To my parents

ABSTRACT

WEI HUANG. Frame Wavelets in High Dimension. (Under the direction of DR. XINGDE DAI)

In this dissertation, the classic one dimension orthogonal wavelet construction scheme is discussed and extended to construct Parseval's frame wavelets in high dimension scenario. An iterative algorithm is developed to construct various Parseval's frame wavelets, where the input is a set of wavelet coefficients which satisfies the associated Lawton's System of Equations.

The relation between one dimension and high dimension wavelet coefficients is explored. Examples are given, showing that, it is possible to use existing one dimension wavelet coefficients to form high dimension versions, with purposeful rearrangement of the terms of the wavelet coefficients that satisfy both one dimension and high dimension Lawton's System of Equations associated with. And it follows that one can obtain one dimension wavelet coefficients sets from high dimension versions.

Applications of Parseval's frame wavelets in signal processing are discussed. Unlike the classic axis-by-axis discrete wavelet transform method, a different quincunx downsampling approach is proposed in the two dimension image processing scenario, with the use of a quincunx sub-lattice.

ACKNOWLEDGMENTS

I would never have been able to finish my dissertation without the guidance of my committee members, help from friends, and support from my family.

Here I would like to express my deepest gratitude to my advisor, Dr. Xingde Dai, for his excellent guidance, caring, patience, and continuous support of my Ph.D study. I would like to thank Dr. Yuanan Diao for his insightful comments and encouragement during countless discussions throughout my research work. I would also like to thank Dr. Evan Houston for his inspiring algebra classes, which helped me to develop my background and deepened my understanding in mathematics. Special thanks goes to Dr. Wei Zhao, who was willing to participate in my final defense committee in short notice.

My sincere thanks also goes to Dr. Joel Avrin, Dr. Mohammad Kazemi and Dr. Shaozhong Deng for caring and support during my Ph.D studies.

TABLE OF CONTENTS

LIST OF FIGURES

LIST OF TABLES

CHAPTER 1: INTRODUCTION: WAVELET THEORY

A wavelet, meaning "small wave", is an oscillation that resembles a wave with an amplitude that begins at zero, increases, and then decreases back to zero. Alfred Haar in [5] introduced the very first wavelet function, known now as the Haar wavelet, is a "square-shaped" function defined as $\psi_H \equiv \chi_{[0,\frac{1}{2})} - \chi_{[\frac{1}{2},1)}$. Its graph is illustrated in Figure (1).

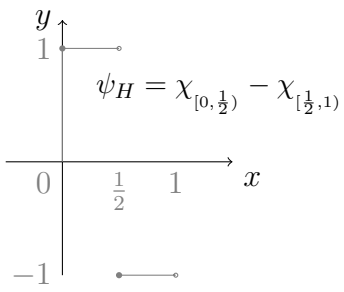

Figure 1: Haar Wavelet

Usually, A set of wavelets(or called "a wavelet family") is purposefully crafted with specific properties, and then are combined with input signals, using a technique called "convolution", to decompose the original input without gaps or overlap into different components, thus facilitates the study of each component. This decomposition process is mathematically reversible, that means, when one wants to recover the original signal with minimal loss, wavelet based compression/decompression algorithms can be utilized with these wavelets.

In the field of signal processing, the application of wavelets are referred as wavelet

transform. One can apply wavelet transform on many different kinds of signal data, most common ones are audio/video signals and images.

We distinguish between the two wavelet transform: Continuous wavelet transform and Discrete wavelet transform. In this dissertation, we will focus on the discrete wavelet transform. More detailed discussions regarding continuous wavelet transform can be found in [6]. Discrete wavelet transform has two different categories: Orthonormal bases of wavelets and redundant systems(called frame wavelets). We will discuss both categories with an emphasis on the latter.

1.1 Unitary Operators in Hilbert Space

We first introduce some notations that are used throughout the dissertation.

In a Hilbert space $\mathbb{H} = \mathrm{L}^2(\mathbb{R})$, let T_α be the "translation-by-α" operator and D the "dilation-by-2"(*dyadic*) operator acting on $\mathbb{H}$ defined by

$$T_\alpha f(t) = f(t-\alpha);\ Df(t) = \sqrt{2}f(2t),\ \forall f \in \mathrm{L}^2(\mathbb{R}), \tag{1}$$

where α is an arbitrary real number. In particular, denote $T = T_1$ when $\alpha = 1$. Let $M_{e^{-i\alpha s}}$ be the multiplication operator by $e^{-i\alpha s}$. T_α, D and $M_{e^{-i\alpha s}}$ are unitary operators in $\mathfrak{B}(\mathbb{H})$, the space of all bounded linear operators on $\mathbb{H}$.

Remark 1.1. *While "dilation-by-m" operators in $\mathbb{H}$ are well defined for arbitrary $m \geq 2$, this dissertation will only focus on dyadic dilation operators.*

Let $\mathcal{F}$ be the Fourier transform on $\mathbb{H} = \mathrm{L}^2(\mathbb{R})$. If $f, g \in \mathrm{L}^2(\mathbb{R}) \bigcap \mathrm{L}^2(\mathbb{R})$, then

$$(\mathcal{F}f)(s) = \frac{1}{\sqrt{2\pi}} \int_{\mathbb{R}} e^{-ist} f(t)dt = \hat{f}(s),$$
$$(\mathcal{F}^{-1}g)(t) = \frac{1}{\sqrt{2\pi}} \int_{\mathbb{R}} e^{ist} g(s)ds = \check{g}(t).$$

We write

$$\widehat{T}_\alpha = \mathcal{F}T_\alpha\mathcal{F}^{-1};\ \widehat{D} = \mathcal{F}D\mathcal{F}^{-1}, \tag{2}$$

then

$$\begin{aligned}(\widehat{T}_\alpha \hat{f})(s) &= (\mathcal{F}T_\alpha f)(s) \\ &= \frac{1}{\sqrt{2\pi}} \int_{\mathbb{R}} e^{-ist} f(t-\alpha)dt = (e^{-i\alpha s}\hat{f})(s), \\ (\widehat{D}\hat{f})(s) &= (\mathcal{F}Df)(s) \\ &= \frac{1}{\sqrt{2\pi}} \int_{\mathbb{R}} e^{-ist}\sqrt{2} f(2t)dt = (D^{-1}\hat{f})(s).\end{aligned}$$

so

$$\widehat{T}_\alpha = M_{e^{-i\alpha s}};\ \widehat{D} = D^{-1}. \tag{3}$$

For $f \in \mathrm{L}^2(\mathbb{R})$, we have

$$(T_\alpha D f)(t) = T_\alpha(\sqrt{2} f(2t)) = \sqrt{2} f(2(t-\alpha)) = \sqrt{2} f(2t-2\alpha) = (DT_\alpha^2 f)(t),$$

so

$$T_\alpha D = DT_\alpha^2. \tag{4}$$

This as well as (2) implies that

$$\widehat{T}_\alpha \widehat{D} = \widehat{D}\widehat{T}_\alpha^2. \tag{5}$$

In the high-dimensional scenario, say, $\mathbb{H} = \mathrm{L}^2(\mathbb{R}^d), d \geq 2$, we have similar notations.

Unlike the 1-dimensional case, we can no longer define the dilation-by-2 operator with "multiply-by-2". Instead, we need matrices:

Definition 1.1. *A $d \times d$ matrix A is **integral** if all its entries are integers and is **expansive** if all its eigenvalues have norm greater than* 1.

We can define the unitary operators $T_{\vec{k}}$ and D_A acting on $\mathbb{H} = \mathrm{L}^2(\mathbb{R}^d)$ as follows:

Definition 1.2. *Let A be an integral expansive matrix, $\forall f \in \mathrm{L}^2(\mathbb{R}^d)$, we define*

$$T_{\vec{k}} f(\vec{t}) = f(\vec{t} - \vec{k});\ \forall \vec{k} \in \mathbb{Z}^d$$

$$D_A f(\vec{t}) = |\det A|^{\frac{1}{2}} f(A\vec{t}).$$

$T_{\vec{k}}$ is the "translation-by-$\vec{k}$" operator and D_A is the "dilation-by-A" operator. They are both unitary operators in $\mathbb{H}$.

One last unitary operator we will use in this dissertation is defined as follows:

Definition 1.3. *Let S be and integral matrix with $|\det S| = 1$, define*

$$U_S f(\vec{t}) = f(S\vec{t}),\ \forall f \in \mathrm{L}^2(\mathbb{R}^d). \tag{6}$$

1.2 Frames and Orthonormal Bases of Hilbert Space

We introduce some useful concepts in the Hilbert space $\mathbb{H}$.

Definition 1.4. *A set of elements $\{\psi_i\}$ is called a **frame** of $\mathbb{H}$ if there exist two positive constants $0 < A \leq B$ such that*

$$A\|f\|^2 \leq \sum_i |\langle f, \psi_i \rangle|^2 \leq B\|f\|^2 \ , \ \forall f \in \mathbb{H},$$

where $\langle \cdot, \cdot \rangle$ is the inner product.

*The supremum of all such numbers A and the infimum of all such numbers B are called the **frame bounds** of the frame and are denoted as A_0 and B_0. $\{\psi_i\}$ is called a **tight frame** if $A_0 = B_0$.*

*In particular, $\{\psi_i\}$ is called a **normalized tight frame**(or **Parseval's frame**) if $A_0 = B_0 = 1$, since it satisfies the Parseval's identity*

$$\sum_i |\langle f, \psi_i \rangle|^2 = \|f\|^2 \ , \ \forall f \in \mathbb{H},$$

which is equivalent to

$$f = \sum_i \langle f, \psi_i \rangle \psi_i \ , \ \forall f \in \mathbb{H}.$$

Definition 1.5. *A set of elements $\{\psi_i\}$ is **orthogonal** if*

$$\langle \psi_i, \psi_j \rangle = 0, i \neq j.$$

If a Parseval's frame is also orthogonal, then it is an **orthonormal basis** for $\mathbb{H}$. And Parseval's identity holds for any orthonormal basis $\{\psi_i\}$.

Now we see that Parseval's frames can play the role of orthonormal bases in the

sense that they satisfy the Parseval's identity, while not required to be orthogonal. We will enjoy this flexibility in the construction of wavelets as this leads to a new type of wavelets — the non-orthonormal bases wavelets, or frame wavelets.

With the unitary operators introduced earlier, we can definite a discrete set of wavelets from the Haar wavelet ψ_H as following:

$$\{\psi_{j,k} \ ; \ j,k \in \mathbb{Z}\} = \{D^j T^k \psi_H \ ; \ j,k \in \mathbb{Z}\} \tag{7}$$

It is easy to verify that $\{\psi_{j,k} \ ; \ j,k \in \mathbb{Z}\}$ is an orthonormal basis for the Hilbert space $\mathrm{L}^2(\mathbb{R})$.

For any $f \in \mathrm{L}^2(\mathbb{R})$, we can further definite its discrete wavelet coefficients as

$$\langle f, \psi_{j,k} \rangle \ ; \ j,k \in \mathbb{Z} \tag{8}$$

The motivation of wavelet theory is shown here: we can approximate an arbitrary function $f \in \mathrm{L}^2(\mathbb{R})$ by a finite linear combinations of the set of wavelets that is derived from the Haar wavelet(or any other wavelets), since f is completely characterized by its discrete wavelet coefficients. On the other hand, it is possible to recover f from its discrete wavelet coefficients. That means, $\mathrm{L}^2(\mathbb{R})$ is spanned by the discrete set of wavelets $\{\psi_{j,k} \ ; \ j,k \in \mathbb{Z}\}$.

Before we continue, let's visit a useful concept of certain structures on $\mathrm{L}^2(\mathbb{R})$: **Multiresolution analysis**(or **MRA** for short), an elegant framework for wavelet construction formulated by Y.Meyer [10] and S.Mallat [9].

Definition 1.6. *The pair of functions* $(\varphi, \ \psi)$ *is called an* ***orthogonal*** *MRA-pair if*

1. *$\{T^k\varphi \ ; \ k \in \mathbb{Z}\}$ and $\{T^k\psi \ ; \ k \in \mathbb{Z}\}$ are orthogonal sets.*

2. *Let $V^{(0)} \equiv span(\{T^k\varphi \ ; \ k \in \mathbb{Z}\})$ and $V^{(n)} \equiv D^n V^{(0)}$.*

   We have $V^{(n)} \subset V^{(n+1)} \ ; \ n \in \mathbb{Z}$

3. *$\overline{\bigcup V^{(n)}} = L^2(\mathbb{R})$ and $\bigcap_{n\in\mathbb{Z}} V^{(n)} = \{0\}$.*

4. *Let $\psi \in W^{(0)} \equiv V^{(1)} \ominus V^{(0)}$, then $\{T^k\psi \ ; \ k \in \mathbb{Z}\}$ is an orthonormal basis of $W^{(0)}$.*

φ and ψ are called the **scaling function** and the **wavelet function** for the MRA, respectively. By the above definition, it is clear that $\{D^nT^k\psi \ ; \ n, k \in \mathbb{Z}\}$ is an orthonormal basis for $L^2(\mathbb{R})$. Moreover, $\{D^nT^k\psi \ ; \ k \in \mathbb{Z}\}$ is an orthonormal basis for $W^{(n)}$ for $n \in \mathbb{Z}$ and $\{D^nT^k\varphi \ ; \ k \in \mathbb{Z}\}$ is an orthonormal basis for $V^{(n)}$ for $n \in \mathbb{Z}$.

In the case of Haar wavelet, it is easy to verify that $(\phi_H \equiv \chi_{[0,1)}, \ \psi_H)$ is an orthogonal MRA-pair. The graphs is shown in Figure (2).

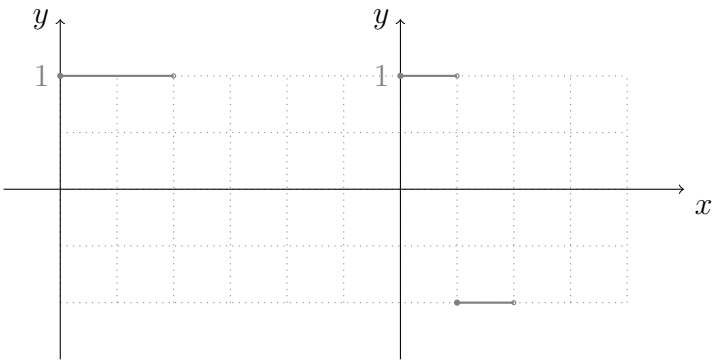

Figure 2: Scaling function and Wavelet function of Haar Wavelet

The scaling function φ satisfies the so called two-scale relation:

$$\varphi(x) = \sqrt{2}\sum_n h_n\varphi(2x-n) = \left(\sum_n h_n DT^n\varphi\right)(x), \tag{9}$$

where $\{h_n\}$ are the coefficients that can be obtained as [1]

$$h_n \equiv \langle \varphi, DT^n \varphi \rangle. \tag{10}$$

Among many possible choices of wavelet function ψ, there exists one that satisfies

$$g_n \equiv \langle \psi, DT^n \varphi \rangle = (-1)^n \cdot \overline{h_{1-n}}. \tag{11}$$

We can write the previous one into the following equivalent form:

$$\psi(x) = \left(\sum_n g_n DT^n \varphi \right)(x). \tag{12}$$

In the previous section, we defined an **orthogonal** MRA, where the orthonormality of $\{T^k \varphi \ ; \ k \in \mathbb{Z}\}$ is required. As a matter of fact, this requirement can be relaxed: if $\{T^k \varphi \ ; \ k \in \mathbb{Z}\}$ is a Parseval's frame, we can define a generalized MRA (in [7])/frame MRA (in [1]) as follows:

Definition 1.7. *The pair of functions $\{\varphi, \ \psi\}$ is called an MRA-pair if*

1. *Let $V^{(0)} \equiv span(\{T^k \varphi \ ; \ k \in \mathbb{Z}\})$ and $V^{(n)} \equiv D^n V^{(0)}$.*

   We have $V^{(n)} \subset V^{(n+1)} \ ; \ n \in \mathbb{Z}$

2. *$\overline{\bigcup V^{(n)}} = L^2(\mathbb{R})$ and $\bigcap_{n \in \mathbb{Z}} V^{(n)} = \{0\}$.*

3. *If $\{T^k \varphi \ ; \ k \in \mathbb{Z}\}$ and $\{T^k \psi \ ; \ k \in \mathbb{Z}\}$ are Parseval's frames in V_0 and W_0, respectively, then $\{D^j T^k \psi \ ; \ j, k \in \mathbb{Z}\}$ is a Parseval's frame in $\mathrm{L}^2(\mathbb{R})$.*

This concepts can be easily extended to high dimension with the use of matrices:

[1] For Haar wavelet, we have $\{h_0 = h_1 = \frac{\sqrt{2}}{2}\}$.

Definition 1.8. *Let A be a $d \times d$ expansive integral matrix with $|\det A| = 2$ and $\varphi,\ \psi$ be two functions in $L^2(\mathbb{R}^d)$. Denote*

$$V_A^{(0)} \equiv span(\{T_{\vec{\ell}}\,\varphi, \vec{\ell} \in \mathbb{Z}^d\}).$$

$$V_A^{(n)} \equiv D_A^n V_A^{(0)}, n \in \mathbb{Z}.$$

The pair of functions $\{\varphi,\ \psi\}$ is called an MRA-pair associated with matrix A if

1. $V_A^{(n)} \subset V_A^{(n+1)},\ n \in \mathbb{Z}$.
2. $\overline{\bigcup_{n\in\mathbb{Z}} V_A^{(n)}} = L^2(\mathbb{R}^d)$ *and* $\bigcap_{n\in\mathbb{Z}} V_A^{(n)} = \{0\}$.
3. $\psi \in V_A^{(1)}$ *is a Parseval's frame wavelet for* $L^2(\mathbb{R}^d)$ *associated with matrix* A.

Q. Gu and D. Han in [11] proved that, if an integral expansive matrix associates with a single function orthogonal wavelets with MRA, then the absolute value of the matrix determinant must be 2. This dissertation studies wavelets associated with MRAs, thus the matrix A in discussion all satisfies $|\det A| = 2$.

1.3 Wavelet Decomposition and Reconstruction of Functions

Within the orthogonal MRA framework, we are ready to introduce a fast cascading wavelet algorithm that is widely used signal analysis to decompose as well as reconstruct functions in $\mathrm{L}^2(\mathbb{R})$.

Let $(\varphi,\ \psi)$ be an orthogonal MRA-pair as defined earlier.

First let's establish the change-of-basis formulas between the MRA layer. Recall that $\{T^k\varphi(x)\ ;\ k\in\mathbb{Z}\}$ and $\{T^k\psi(x)\ ;\ k\in\mathbb{Z}\}$ are the bases in V_0 an W_0. We have

$$\begin{aligned} T^k\varphi(x) &= T^k\sum_n h_n DT^n\varphi(x) \text{ (by (9))} \\ &= \sum_n h_n T^k DT^n\varphi(x) = \sum_n h_n DT^{2k}T^n\varphi(x) \text{ (by (4))} \\ &= \sum_n h_n DT^{n+2k}\varphi(x) = \sum_n h_{n-2k} DT^n\varphi(x) \end{aligned}$$

$$\begin{aligned} T^k\psi(x) &= T^k\sum_n g_n DT^n\varphi(x) \text{ (by (12))} \\ &= \sum_n g_n T^k DT^n\varphi(x) = \sum_n g_n DT^{2k}T^n\varphi(x) \text{ (by (4))} \\ &= \sum_n g_n DT^{n+2k}\varphi(x) = \sum_n g_{n-2k} DT^n\varphi(x) \end{aligned}$$

That is

$$\begin{cases} T^k\varphi(x) = \sum_n h_{n-2k} DT^n\varphi(x); \\ T^k\psi(x) = \sum_n g_{n-2k} DT^n\varphi(x). \end{cases} \tag{13}$$

Apply D^{j-1} on both sides, we obtain the following change-of-basis formulas from

V_j to V_{j-1} and W_{j-1}, for $j \in \mathbb{Z}$:

$$\begin{cases} D^{j-1}T^k\varphi(x) = D^{j-1}\sum_n h_{n-2k}DT^n\varphi(x) = \sum_n h_{n-2k}D^jT^n\varphi(x); \\ D^{j-1}T^k\psi(x) = D^{j-1}\sum_n g_{n-2k}DT^n\varphi(x) = \sum_n g_{n-2k}D^jT^n\varphi(x), \end{cases} \tag{14}$$

Next, define P_j as the orthogonal projection onto V_j, and Q_j the orthogonal projection onto W_j, where V_j and W_j are the subspaces in this MRA for $j \in \mathbb{Z}$.

Since $V_j \subset V_{j+1}, j \in \mathbb{Z}$, we understand that V_j is a "coarser" version of V_{j+1}.

For an arbitrary function $f \in \mathrm{L}^2(\mathbb{R})$, we start out with the finest-scale approximation to f, $f^J = P_J f \in V_J$. In practice, we just treat f^J as f itself, as f^J is the best we can do to characterize f. Note that, while the choice of J is arbitrary, we usually pick J as some positive integer and restrict our attention to only V_j's and W_j's for $j \leq J$.

Now, we can represent f^J as:

$$f^J = \sum_k c_k^J D^J T^k \varphi,$$

where $\{c_k^J \ ; \ k \in \mathbb{Z}\}$ is the discrete wavelet coefficients which can be defined as

$$c_k^J = \langle f^J, D^J T^k \varphi \rangle.$$

In practice, the actual input signal information is treated as $\{c_k^J \ ; \ k \in \mathbb{Z}\}$. That is, the function f is introduced here only as a utility function and we don't really care about its actual values except for its discrete wavelet coefficients in V_J, which is $\{c_k^J \ ; \ k \in \mathbb{Z}\}$.

The center of the decomposition process is: we want to find f's discrete wavelet coefficients in the next level of the MRA, given its discrete wavelet coefficients $\{c_k^J \ ; \ k \in$

$\mathbb{Z}\}$ in V_J.

For f, denote $\{c_k^j \ ; \ k \in \mathbb{Z}\}$ as its discrete wavelet coefficients in V_j and $\{d_k^j \ ; \ k \in \mathbb{Z}\}$ as its discrete wavelet coefficients in W_j. Apply the change-of-basis formulas in (14), we have

$$\begin{aligned}
c_k^{J-1} &= \langle f^{J-1}, D^{J-1}T^k\varphi\rangle \\
&= \langle P_{j-1}f^J, D^{J-1}T^k\varphi\rangle \\
&= \langle f^J, P_{j-1}^* D^{J-1}T^k\varphi\rangle \\
&= \langle f^J, D^{J-1}T^k\varphi\rangle \\
&= \langle f^J, \sum_n h_{n-2k} D^J T^n\varphi\rangle \\
&= \sum_n \overline{h_{n-2k}}\langle f^J, D^J T^n\varphi\rangle \\
&= \sum_n \overline{h_{n-2k}} c_n^J; \\
d_k^{J-1} &= \langle f^{J-1}, D^{J-1}T^k\psi\rangle \\
&= \langle P_{j-1}f^J, D^{J-1}T^k\psi\rangle \\
&= \langle f^J, P_{j-1}^* D^{J-1}T^k\psi\rangle \\
&= \langle f^J, D^{J-1}T^k\psi\rangle \\
&= \langle f^J, \sum_n g_{n-2k} D^J T^n\varphi\rangle \\
&= \sum_n \overline{g_{n-2k}}\langle f^J, D^J T^n\varphi\rangle \\
&= \sum_n \overline{g_{n-2k}} c_n^J.
\end{aligned}$$

This shows a hierarchical and fast way to compute the wavelet coefficients of a

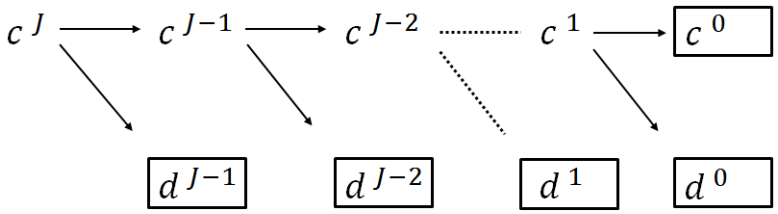

Figure 3: Cascading Scheme – Decomposition

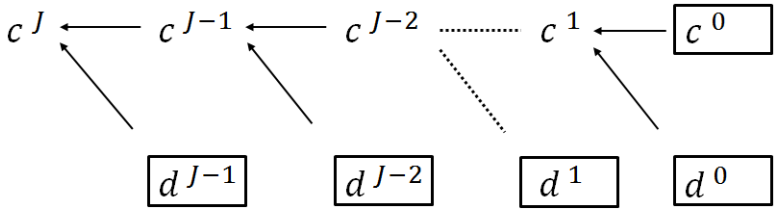

Figure 4: Cascading Scheme – Reconstruction

given function: start with the finest-scale level J, we have the wavelet coefficients c^J, which fully characterized f in V_J. Then we calculate c^{J-1} and d^{J-1}, the next(coarser) level's wavelet coefficients. By doing that, we successfully decomposed the original functions information c^J into two part: the coarser version of it — c^{J-1}, and the difference(or details) of the information between two successive levels — d^{J-1}. We can repeat this process for multiple levels.

In practice, we will stop after a finite number of levels.

If we start at level J and stops at level 0, we will decompose c^J into a final coarse approximation c^0 and a serial of details $d^{J-1}, d^{J-2}, ..., d^2, d^1, d^0$. The decomposition schema is illustrated in Figure (3) and the following formulas are the decomposition formulas:

$$\begin{cases} c_k^{j-1} = \sum_n \overline{h_{n-2k}} c_n^j; \\ d_k^{j-1} = \sum_n \overline{g_{n-2k}} c_n^j. \end{cases} \tag{15}$$

On the other hand, given a final coarse approximation c^0 and a serial of details $d^{J-1}, d^{J-2}, ..., d^2, d^1, d^0$, we do have a reconstruction schema that can restore the

exact original information c^J. The basic idea is illustrated in Figure (4). And the reconstruction formula is:

$$c_n^j = \sum_k \left[h_{n-2k} c_k^{j-1} + g_{n-2k} d_k^{j-1} \right]. \tag{16}$$

This fast wavelet decomposition and reconstruction algorithm for discrete wavelet transform(DWT), first proposed by Mallat in [9], is, in fact, a classical scheme in the signal processing community, known as a two-channel subband coder using conjugate quadrature filters or quadrature mirror filters (QMFs).

In Chapter 4, we will discuss this topic in more details with examples.

Till now, it might seem like the very first thing we need to have is the scaling function φ or the wavelet function ψ before we can get the coefficients set $\{h_n\}$. Luckily, this is not the case. We could obtain the coefficients set $\{h_n\}$ somewhere else and construct everything including φ and ψ from it. The whole process, a frame wavelet construction scheme, and its natural extension to high dimension, is the center of this dissertation.

CHAPTER 2: CONSTRUCTION OF PARSEVAL'S FRAMES

2.1 Construct Frames in $L^2(\mathbb{R})$

We will illustrate a construction scheme in $L^2(\mathbb{R})$ for Parseval's frame wavelets with compact support. This approach, proposed by Lawton[13] and Daubechies[6], can provide all Parseval's frame wavelets in the 1-dimensional case. In following chapters, we will extend this approach to d-dimensional cases.

We start with a system of equations that later referred as **Lawton's System of Equations**. Let $\{h_n\ ;\ n \in \mathbb{Z}\}$ be a complex solution to the following Lawton's System of Equations:

$$\begin{cases} \sum_{n\in\mathbb{Z}} h_n \overline{h_{n+k}} = \delta_{0k},\ k \in 2\mathbb{Z} \\ \sum_{n\in\mathbb{Z}} h_n = \sqrt{2}. \end{cases} \tag{17}$$

Assume further that this solution has only finite many nonzero elements. That is, for some fixed odd integer $N \in \mathbb{Z}^+$, $h_n = 0$ if $n < 0$ or $n > N$. In such case, $|h_n| \leq M_c$ for some $M_c \in \mathbb{R}^+$ when $0 \leq n \leq N$.

Choose an element $q = 1 \in \mathbb{Z}$, we have $\mathbb{Z} = 2\mathbb{Z} \bigcup (2\mathbb{Z} + q)$. We call $2\mathbb{Z}$ a sub-lattice of $\mathbb{Z}$.

Define a trigonometric polynomial function m_0:

$$m_0(\xi) = \frac{1}{\sqrt{2}} \sum_{n=0}^{N} h_n e^{-in\xi}. \tag{18}$$

This is a 2π-periodic function with $m_0(0) = 1$. It is called the **filter function**.

Next, define

$$g(\xi) = (2\pi)^{-1/2} \prod_{j=1}^{\infty} m_0(2^{-j}\xi); \varphi = \mathcal{F}^{-1} g.$$

$g(\xi)$ is a $\mathrm{L}^2(\mathbb{R})$-function and its extension is an entire function on $\mathbb{C}$. And the **scaling function** $\varphi(x)$ is a $\mathrm{L}^2(\mathbb{R})$-function with compact support and satisfies the two-scale relation:

$$\varphi(x) = \sqrt{2} \sum_{n=0}^{N} h_n \varphi(2x - n) = \left(\sum_{n=0}^{N} h_n D T^n \varphi \right)(x). \tag{19}$$

Finally, define the **wavelet function** ψ as

$$\psi(x) = \sqrt{2} \sum_{n=0}^{N} (-1)^n \overline{h_{-n+N}} \varphi(2x - n) = \left(\sum_{n=0}^{N} (-1)^n \overline{h_{-n+N}} D T^n \varphi \right)(x), \tag{20}$$

and $\{\psi_{j,k} \ ; \ j,k \in \mathbb{Z}\} = \{D^j T^k \psi \ ; \ j,k \in \mathbb{Z}\}$ constitute a Parseval's frame for $\mathrm{L}^2(\mathbb{R})$.

Detailed discussion and proofs for the above construction scheme can be found in literature [13] and [6]. We completed a proof for this approach with the use of unitary operator notations, but we omit it here since we will provide a proof for a more generalized, high dimension version of this construction scheme.

2.2 Construct Frames in $L^2(\mathbb{R}^d)$

2.2.1 Construction Scheme

In this section, we extend the construction scheme to the high dimension.

First we introduce the Partition Theorem for $d \times d$ expansive integral matrices from [3].

Theorem 2.1. ***Partition Theorem***

Every integral matrix B with $|\det(B)| = 2$ is integrally similar to an integral matrix A with the properties that

1. $$A\mathbb{Z}^d = A^\tau \mathbb{Z}^d.$$

2. *There exists a vector $\vec{\ell}_A \in \mathbb{Z}^d$ such that*

$$\mathbb{Z}^d = (\vec{\ell}_A + A\mathbb{Z}^d) \dot{\cup} A\mathbb{Z}^d.$$

3. *There exists a vector $\vec{q}_A \in \mathbb{Z}^d$*

$$\vec{q}_A \circ A\mathbb{Z}^d \subseteq 2\mathbb{Z} \quad \textit{and} \quad \vec{q}_A \circ (\vec{\ell}_A + A\mathbb{Z}^d) \subseteq 2\mathbb{Z} + 1.$$

4. *For $\vec{m} \in A\mathbb{Z}^d$, we have*

$$\mathbb{Z}^d = (\vec{n} - A\mathbb{Z}^d) \dot{\cup} (\vec{\ell}_A - \vec{m} - \vec{n} + A\mathbb{Z}^d), \ \forall \vec{n} \in \mathbb{Z}^d.$$

5. *For $\vec{m} \in \vec{\ell}_A + A\mathbb{Z}^d$, we have*

$$\vec{n} - A\mathbb{Z}^d = \vec{\ell}_A - \vec{m} - \vec{n} + A\mathbb{Z}^d, \ \forall \vec{n} \in \mathbb{Z}^d.$$

When $d = 2$, Dai in [2] states that, each expansive integral matrix with determinant ± 2 is integrally similar to one of the following 6 matrices:

$$\begin{bmatrix} 1 & 1 \\ 1 & -1 \end{bmatrix}, \begin{bmatrix} 1 & -3 \\ 1 & -1 \end{bmatrix}, \begin{bmatrix} 1 & 1 \\ -1 & 1 \end{bmatrix}, \begin{bmatrix} -1 & -1 \\ 1 & -1 \end{bmatrix}, \begin{bmatrix} -1 & 2 \\ -2 & 2 \end{bmatrix}, \begin{bmatrix} 1 & -2 \\ 2 & -2 \end{bmatrix}. \quad (21)$$

Each of the above 6 matrix satisfies the 5 properties mentioned in Partition Theorem (Theorem 2.1).

Let A_0 be a $d \times d$ expansive integral matrix with $|\det(A_0)| = 2$. We will construct Parseval's frame wavelets associated with A_0 in the following 5 steps.

Step 1. Find a $d \times d$ integral matrix A from the 6 matrices in (21), which is integrally similar to A_0 with the following properties:

1. $$S^{-1}AS = A_0,$$

   where S is an integral matrix with $|\det(S)| = 1$.

2. $$A\mathbb{Z}^d = A^\tau \mathbb{Z}^d,$$

   where A^τ is the transpose of A.

3. There exists a vector $\vec{\ell}_A \in \mathbb{Z}^d$ such that

   $$\mathbb{Z}^d = (\vec{\ell}_A + A\mathbb{Z}^d) \cup A\mathbb{Z}^d.$$

4. There exists a vector $\vec{q}_A \in \mathbb{Z}^d$

$$\vec{q}_A \circ A\mathbb{Z}^d \subseteq 2\mathbb{Z} \quad and \quad \vec{q}_A \circ (\vec{\ell}_A + A\mathbb{Z}^d) \subseteq 2\mathbb{Z} + 1.$$

Step 2. Solve Lawton's System of Equations

$$\begin{cases} \sum_{\vec{n}\in\mathbb{Z}^d} h_{\vec{n}}\overline{h_{\vec{n}+\vec{k}}} = \delta_{\vec{0}\vec{k}},\ \vec{k} \in A\mathbb{Z}^d \\ \sum_{\vec{n}\in\mathbb{Z}^d} h_{\vec{n}} = \sqrt{2}. \end{cases}$$

for a finite solution $\mathcal{S} = \{h_{\vec{n}} : \ \vec{n} \in \mathbb{Z}^d\}$. We say $\mathcal{S}$ is a finite solution if the index set of non-zero terms $h_{\vec{n}}$ is included in the set $\Lambda_0 \equiv \mathbb{Z}^d \cap [-N_0, N_0]^d$ for some natural number N_0.

Step 3. Let Ψ be the linear operator on $L^2(\mathbb{R}^d)$:

$$\Psi \equiv \sum_{\vec{n}\in\Lambda_0} h_{\vec{n}} D_A T_{\vec{n}}.$$

The iterated sequence $\{\Psi^k \chi_{[0,1)^d}, k \in \mathbb{N}\}$ will converge to the scaling function φ_A in the $L^2(\mathbb{R}^d)$-norm (Theorem 10.2 in [3]).

φ_A satisfies the two-scale relation:

$$\varphi_A = \sum_{\vec{n}\in\Lambda_0} h_{\vec{n}} D_A T_{\vec{n}} \varphi_A. \tag{22}$$

Step 4. Define function ψ_A

$$\psi_A \ \equiv \ \sum_{\vec{n}\in\mathbb{Z}^d} (-1)^{\vec{q}_A \circ \vec{n}} \overline{h_{\vec{\ell}_A - \vec{n}}} D_A T_{\vec{n}} \varphi_A.$$

This is a Parseval's frame wavelet with compact support associated with matrix A (Theorem 9.1 in [3]).

Step 5. Define the wavelet function ψ by

$$\psi(\vec{t}) \equiv U_s \psi_A(\vec{t}) = \psi_A(S\vec{t}), \forall \vec{t} \in \mathbb{R}^d.$$

The function ψ is a Parseval's frame wavelet with compact support associated with the given matrix A_0 (Theorem 5.1 in [3]).

2.2.2 Iterative Algorithm for Wavelet Construction

In this section we will discuss an iterative algorithm that can be used to construct scaling functions and wavelet functions.

Let $f_0(\vec{t})$ be a bounded function in $L^2(\mathbb{R}^d)$ which is contiguous at $\vec{0}$. Define

$$\begin{aligned} g_0(\vec{x}) &\equiv \frac{1}{(2\pi)^{d/2}} \cdot f_0(\vec{x}), \\ g_k(\vec{x}) &\equiv \frac{1}{(2\pi)^{d/2}} \cdot f_0((A^\tau)^{-k}\vec{x}) \cdot \prod_{j=1}^{k} m_0((A^\tau)^{-j}\vec{x}),\ \forall k \geq 1, \end{aligned}$$

and

$$\varphi_k \equiv \mathcal{F}^{-1} g_k, \forall k \geq 0.$$

Since $\lim_k f_0((A^\tau)^{-k}\vec{x})$ is converging to constant function 1 uniformly on any fixed bounded region of $L^2(\mathbb{R}^d)$ and $\prod_{j=1}^{k} m_0((A^\tau)^{-j}\vec{x})$ is also converging uniformly on any fixed bounded region of $L^2(\mathbb{R}^d)$ (see the proof of Proposition 8.1 in [3]).

Hence, we have

$$\varphi_{k+1} = \sum_{\vec{n}\in\Lambda_0} h_{\vec{n}} D_A T_{\vec{n}} \varphi_k,\ k = 1, 2, \cdots,$$

and the first term is

$$\varphi_1 = \sum_{\vec{n}\in\Lambda_0} h_{\vec{n}} D_A T_{\vec{n}} \varphi_0.$$

Let Ψ be the linear operator

$$\Psi \equiv \sum_{\vec{n}\in\Lambda_0} h_{\vec{n}} D_A T_{\vec{n}}. \tag{23}$$

Theorem 10.2 in [3] guarantees the convergence of the above defined linear operator:

Theorem 2.2. *The limit*

$$\lim_{k\to\infty} \Psi^k \chi_{[0,1)^d} = \varphi$$

converges in $L^2(\mathbb{R}^d)$*-norm.*

2.3 Examples in $L^2(\mathbb{R}^2)$

In the first example, we will follow the proposed construction scheme step-by-step to construct a Haar-like frame wavelet.

Example 2.3.1. *A Haar-like frame wavelet in 2D. [12]*

Step 1. *Let* $A_0 \equiv \begin{bmatrix} 0 & 1 \\ 2 & 0 \end{bmatrix}$. *We find that in Partition Theorem, given* $A \equiv \begin{bmatrix} 1 & 1 \\ 1 & -1 \end{bmatrix}, S \equiv \begin{bmatrix} 1 & -1 \\ 0 & 1 \end{bmatrix}$, *we have* $A_0 \equiv S^{-1}AS$.

Obviously, $\vec{\ell}_A \equiv \begin{bmatrix} 1 \\ 0 \end{bmatrix}$ *and* $\vec{q}_A \equiv \begin{bmatrix} 1 \\ 1 \end{bmatrix}$. *Then it is clear that we have* $A = A^\tau$ *and it is left to the reader to check that*

1. $A\mathbb{Z}^2 = A^\tau\mathbb{Z}^2$,
2. $\mathbb{Z}^2 = A^\tau\mathbb{Z}^2 \cup (\vec{\ell}_A + A^\tau\mathbb{Z}^2)$,
3. $A^\tau\mathbb{Z}^2 \circ \vec{q}_A \subset 2\mathbb{Z}$, *and*
4. $(A^\tau\mathbb{Z}^2 + \vec{\ell}_A) \circ \vec{q}_A \subset 2\mathbb{Z} + 1$.

Step 2. *The Lawton's system of equations associated with matrix* A *is*

$$\begin{cases} \sum_{\vec{n}\in\mathbb{Z}^2} h_{\vec{n}}\overline{h_{\vec{n}+\vec{k}}} = \delta_{\vec{0}\vec{k}}, \ \vec{k} \in A^\tau\mathbb{Z}^2 \\ \sum_{\vec{n}\in\mathbb{Z}^2} h_{\vec{n}} = \sqrt{2}. \end{cases} \tag{24}$$

In this example we assume that the only non zero elements are $\vec{n}_0 = [0,0]^\tau$ *and*

$\vec{n}_1 = [1, 0]^\tau$. *The system is*

$$\begin{cases} h_{\vec{n}_0}^2 + h_{\vec{n}_1}^2 = 1 \\ h_{\vec{n}_0} + h_{\vec{n}_1} = \sqrt{2}. \end{cases}$$

We have a solution $h_{\vec{n}_0} = h_{\vec{n}_1} = \frac{\sqrt{2}}{2}$.

Step 3.

By Equation (22) we have the two-scale relation equation on the scaling function φ,

$$\varphi = D_A(h_{\vec{n}_0} I + h_{\vec{n}_1} T_{\vec{n}_1})\varphi = \frac{\sqrt{2}}{2} D_A(I + T_{\vec{n}_1})\varphi. \tag{25}$$

Let Ψ *be the map* $\frac{\sqrt{2}}{2} D_A(I + T_{\vec{n}_1})$, *and* $f_0 = \chi_{[0,1)^2}$, *the characteristic function of two dimensional set* $[0, 1)^2$. *We observe that the sequence* $\{\Psi^n f_0\}$ *approaches to the characteristic function* χ_{Q_A}, *where* Q_A *is the parallelogram with vertices* $\begin{bmatrix} 0 \\ 0 \end{bmatrix}, \begin{bmatrix} 1 \\ 0 \end{bmatrix}, \begin{bmatrix} 2 \\ 1 \end{bmatrix}$ *and* $\begin{bmatrix} 1 \\ 1 \end{bmatrix}$. *Simple calculation shows*

$$\Psi^1 = \left(\frac{\sqrt{2}}{2}\right)(D_A + D_A T_{\vec{n}_1})$$

$$\Psi^2 = \left(\frac{\sqrt{2}}{2}\right)^2 (D_A^2 + D_A^2 T_{\vec{n}_1} + D_A^2 T_{A\vec{n}_1} + D_A^2 T_{A\vec{n}_1 + \vec{n}_1})$$

$$\Psi^3 = \left(\frac{\sqrt{2}}{2}\right)^3 (D_A^3 + D_A^3 T_{\vec{n}_1} + D_A^3 T_{A\vec{n}_1} + D_A^3 T_{A\vec{n}_1 + \vec{n}_1}$$

$$+ D_A^3 T_{A^2\vec{n}_1} + D_A^3 T_{A^2\vec{n}_1 + \vec{n}_1} + D_A^3 T_{A^2\vec{n}_1 + A\vec{n}_1} + D_A^3 T_{A^2\vec{n}_1 + A\vec{n}_1 + \vec{n}_1})$$

...

And the step-by-step iteration results are illustrated in Figure (5). It is clear that the

iterative result is converging to Q_A.

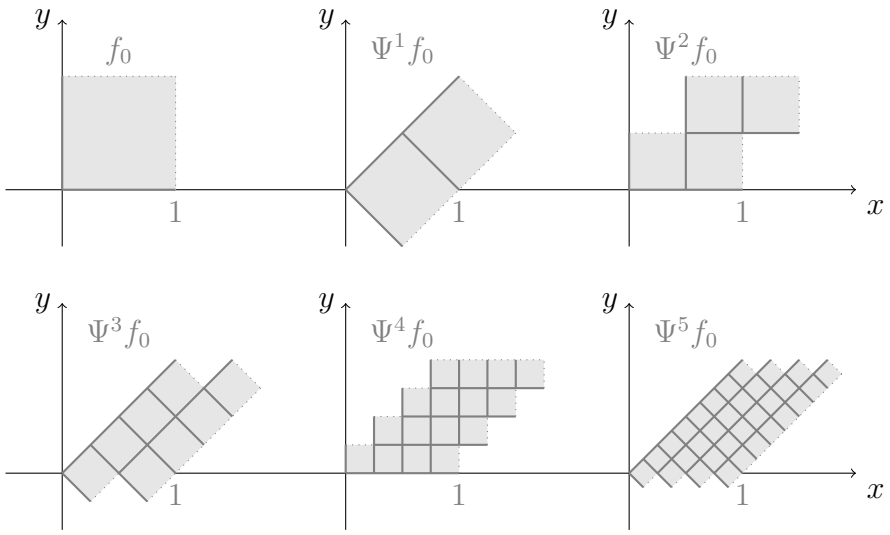

Figure 5: f_0, $\Psi^1 f_0$, $\Psi^2 f_0$, $\Psi^3 f_0$, $\Psi^4 f_0$ and $\Psi^5 f_0$

We denote

$$\varphi_A \equiv \chi_{Q_A}.$$

Step 4. *By Definition the corresponding Parseval's frame wavelet* ψ_A *is*

$$\begin{aligned} \psi_A &\equiv \sum_{\vec{n}\in\mathbb{Z}^d} (-1)^{\vec{q}_A\circ\vec{n}} \overline{h_{\vec{\ell}_A-\vec{n}}} D_A T_{\vec{n}} \varphi_A \\ &= \chi_{Q_A^+} - \chi_{Q_A^-}, \end{aligned}$$

where Q_A^+ *and* Q_A^- *are parallelograms with vertexes* $\left\{ \begin{bmatrix} 0 \\ 0 \end{bmatrix}, \begin{bmatrix} 1 \\ 0 \end{bmatrix}, \begin{bmatrix} 1.5 \\ 0.5 \end{bmatrix}, \begin{bmatrix} 0.5 \\ 0.5 \end{bmatrix} \right\}$ *and* $\left\{ \begin{bmatrix} 0.5 \\ 0.5 \end{bmatrix}, \begin{bmatrix} 1.5 \\ 0.5 \end{bmatrix}, \begin{bmatrix} 2 \\ 1 \end{bmatrix}, \begin{bmatrix} 1 \\ 1 \end{bmatrix} \right\}$, *respectively as showing in Figure (6) and Figure (7). It is easy to check that* $AQ_A^+ = Q_A$.

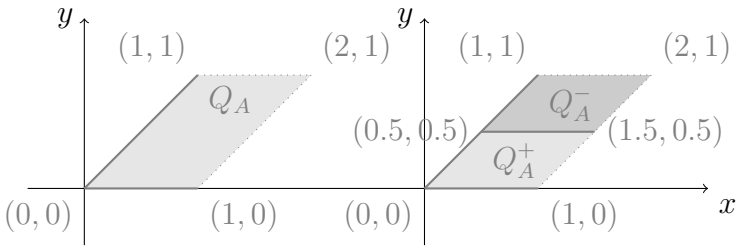

Figure 6: Supports of φ_A and ψ_A

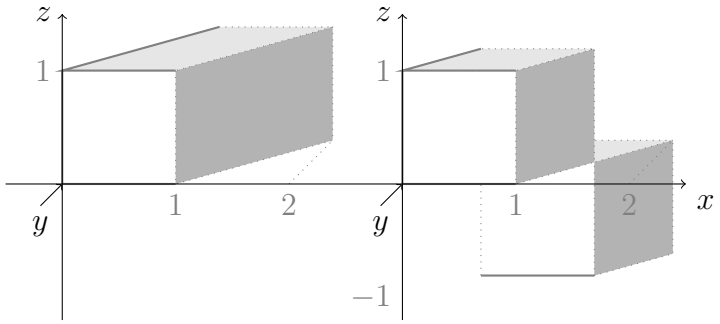

Figure 7: Graphs of φ_A and ψ_A

Step 5. *Define*

$$\varphi_{A_0} \equiv U_S \psi_A,$$

$$\psi_{A_0} \equiv U_S \psi_A.$$

The support and graph of both scaling function φ_{A_0} and wavelet function ψ_{A_0} associated with matrix A_0 are shown in Figure (8) and Figure (9), respectively.

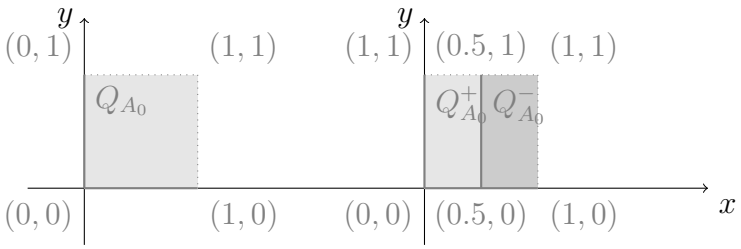

Figure 8: Supports of φ_{A_0} and ψ_{A_0}

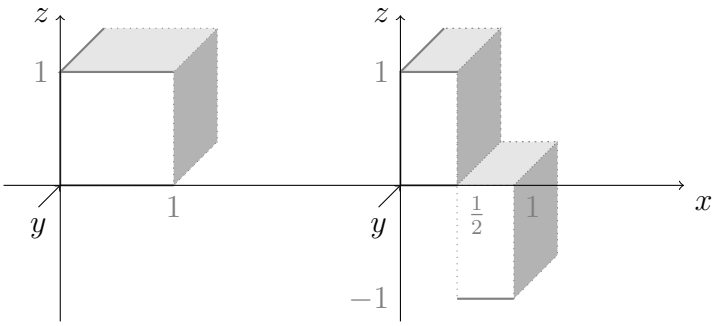

Figure 9: Graphs of φ_{A_0} and ψ_{A_0}

In the next 2 examples, we will present solutions to the Lawton's system of equations that produce known wavelets in the literatures.

Example 2.3.2. *"Resting Dog":*

Let

$$A = \begin{bmatrix} 1 & 1 \\ 1 & -1 \end{bmatrix}, S = \begin{bmatrix} 0 & 1 \\ 1 & -1 \end{bmatrix} \text{ and } A_0 = \begin{bmatrix} 0 & 2 \\ 1 & 0 \end{bmatrix}.$$

Then

$$A_0 = S^{-1}AS$$

We will construct the scaling function φ_A and the related Parseval's frame wavelet ψ_A associated with matrix A. Then, $U_S\varphi_A$ and $U_S\psi_A$ will be the scaling function and Parseval's frame wavelet associated with matrix A_0.

Assume that the support of solution is Λ_0

$$\Lambda_0 = \left\{ \begin{bmatrix} 0 \\ m \end{bmatrix}, m = 0, 1, \cdots, 7 \right\} \cup \left\{ \begin{bmatrix} 1 \\ m \end{bmatrix}, m = -1, 0, \cdots, 6 \right\}$$

The reduced Lawton's system of equations associated with matrix A on Λ_0 has the following 12 *equations:*

$$
\begin{cases}
\sum_{\vec{n}\in\Lambda_0} h_{\vec{n}} & = & \sqrt{2}, \\
\sum_{\vec{n}\in\Lambda_0} h_{\vec{n}}^2 & = & 1, \\
\sum_{k=0}^{5}(h_{0,k}\cdot h_{0,(2+k)} + h_{1,(k-1)}\cdot h_{1,(k+1)}) & = & 0, \\
\sum_{k=0}^{3}(h_{0,k}\cdot h_{0,(4+k)} + h_{1,(k-1)}\cdot h_{1,(k+3)}) & = & 0, \\
\sum_{k=0}^{1}(h_{0,k}\cdot h_{0,(6+k)} + h_{1,(k-1)}\cdot h_{1,(k+5)}) & = & 0, \\
\sum_{k=0}^{7} h_{0,k}\cdot h_{1,(k-1)} & = & 0, \\
\sum_{k=0}^{5} h_{0,k}\cdot h_{1,(k+1)} & = & 0, \\
\sum_{k=0}^{3} h_{0,k}\cdot h_{1,(k+3)} & = & 0, \\
\sum_{k=0}^{1} h_{0,k}\cdot h_{1,(k+5)} & = & 0, \\
\sum_{k=0}^{5} h_{0,(k+2)}\cdot h_{1,(k-1)} & = & 0, \\
\sum_{k=0}^{3} h_{0,(k+4)}\cdot h_{1,(k-1)} & = & 0, \\
\sum_{k=0}^{1} h_{0,(k+6)}\cdot h_{1,(k-1)} & = & 0.
\end{cases}
\tag{26}
$$

Table 1 is a solution to equation system (26). *It is from Table A.*1 *Solution* 2 *of [4]. We rearranged the terms. The solution satisfies the equations* (26) *within errors less than* 10^{-13}.

	$h_{1,-1}$		0.011177337112703
$h_{0,0}$	$h_{1,0}$	0.052282268983427	-0.019359715773096
$h_{0,1}$	$h_{1,1}$	-0.090555546214041	-0.195280287797963
$h_{0,2}$	$h_{1,2}$	-0.080300252489051	0.171377820183894
$h_{0,3}$	$h_{1,3}$	0.195120084182308	0.777712940352809
$h_{0,4}$	$h_{1,4}$	0.003753698026408	0.489561273639764
$h_{0,5}$	$h_{1,5}$	-0.118573529719665	0.113496791518999
$h_{0,6}$	$h_{1,6}$	0.024264285477802	0.065527403135986
$h_{0,7}$		0.014008991752812	

Table 1: A solution to Equations (26)

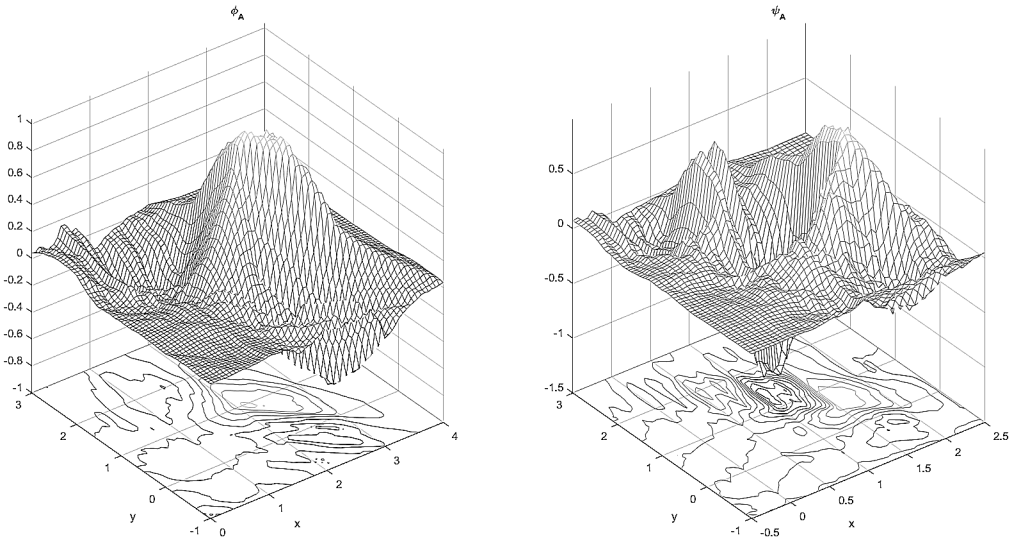

Figure 10: "Resting Dog" Graphs before U_s

Based on this solution, we obtain the corresponding two-scale relation associated with A *and* $\{h_{\vec{n}}, \vec{n} \in \Lambda_0\}$,

$$\varphi_A = \sum_{\vec{n} \in \Lambda_0} h_{\vec{n}} D_A T_{\vec{n}} \varphi_A.$$

Then we obtain the Parseval's frame wavelet function ψ_A *and scaling function* φ_A *associated with* A *by applying the iterative algorithm. The graphs of* φ_A *and* ψ_A *are illustrated in Figure (10).*

Then $\psi_{A_0} \equiv U_S \psi_A$ *and* $\varphi_{A_0} \equiv U_S \varphi_A$ *are the wavelet and scaling function associated with matrix* A_0*. The graphs of* φ_{A_0} *and* ψ_{A_0} *are illustrated in Figure (11). This* φ_{A_0} *is known as the scaling function "Resting Dog" (Fig. 5.2) in [4].*

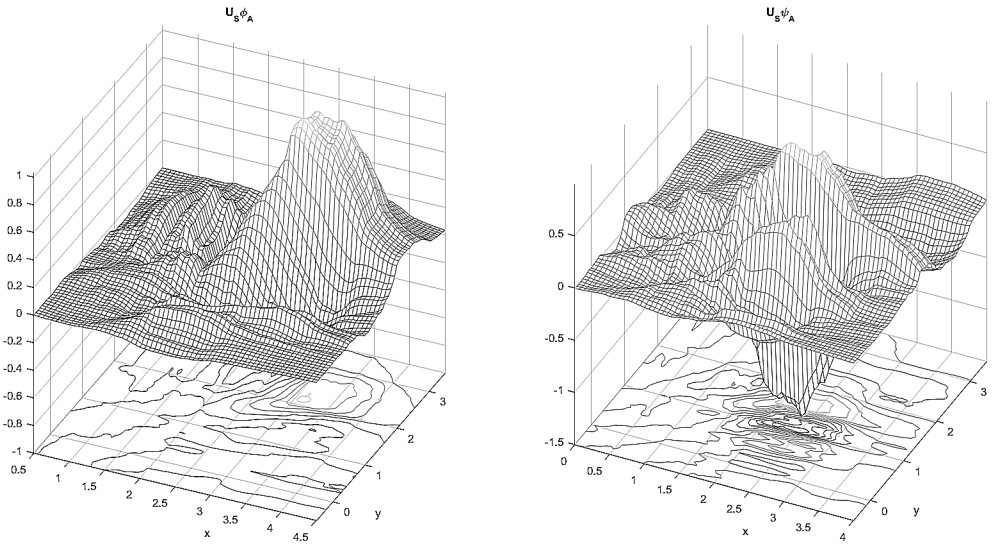

Figure 11: "Resting Dog" Graphs

Example 2.3.3. *"Devil's Tower":*

Let

$$A = \begin{bmatrix} 1 & 1 \\ 1 & -1 \end{bmatrix}, S = \begin{bmatrix} 1 & 1 \\ 1 & 0 \end{bmatrix} \text{ and } A_0 = \begin{bmatrix} 0 & 1 \\ 2 & 0 \end{bmatrix}.$$

Then

$$A_0 = S^{-1}AS$$

We will construct the scaling function φ_A and the related Parseval's frame wavelet ψ_A associated with matrix A. Then, $U_S\varphi_A$ and $U_S\psi_A$ will be the scaling function and Parseval's frame wavelet associated with matrix A_0.

Assume that the support of solution is Λ_0, a 6×2 region:

$$\Lambda_0 = \left\{ \begin{bmatrix} m \\ \\ 0 \end{bmatrix}, m = 0, 1, \cdots, 5 \right\} \cup \left\{ \begin{bmatrix} m \\ \\ 1 \end{bmatrix}, m = 0, \cdots, 5 \right\}$$

The reduced Lawton's system of equations related to Λ_0 associated with matrix A has

the following 10 *equations.*

$$\begin{cases} \sum_{n=0}^{5} h_{n,0} + h_{n,1} & = & \sqrt{2}, \\ \sum_{n=0}^{5} h_{n,0}^2 + h_{n,1}^2 & = & 1, \\ \sum_{n=0}^{3} h_{n,0} \cdot h_{n+2,0} + h_{n,1} \cdot h_{n+2,1} & = & 0, \\ \sum_{n=0}^{1} h_{n,0} \cdot h_{n+4,0} + h_{n,1} \cdot h_{n+4,1} & = & 0, \\ \sum_{n=0}^{0} h_{n,1} \cdot h_{n+5,0} & = & 0, \\ \sum_{n=0}^{2} h_{n,1} \cdot h_{n+3,0} & = & 0, \\ \sum_{n=0}^{4} h_{n,1} \cdot h_{n+5,0} & = & 0, \\ \sum_{n=0}^{4} h_{n,0} \cdot h_{n+1,1} & = & 0, \\ \sum_{n=0}^{2} h_{n,0} \cdot h_{n+3,1} & = & 0, \\ \sum_{n=0}^{0} h_{n,0} \cdot h_{n+5,1} & = & 0. \end{cases} \tag{27}$$

Table 2 is a solution to equation system (27)*. Note that we changed the order of the indices of* h*. The original solution is from "Devil's Tower" Example in [4]. We rearranged the terms to form a solution for the previous system of equations. It satisfies the equations* (27) *within errors less than* 10^{-16}*.*

$h_{0,0}$	$h_{0,1}$	0	0.0473671727453765
$h_{1,0}$	$h_{1,1}$	-0.176776695296637	0.0473671727453765
$h_{2,0}$	$h_{2,1}$	0.176776695296637	0.659739608441171
$h_{3,0}$	$h_{3,1}$	0.176776695296637	0.659739608441171
$h_{4,0}$	$h_{4,1}$	-0.176776695296637	0
$h_{5,0}$	$h_{5,1}$	0	0

Table 2: A solution to Equations (27)

Based on this solution, we obtain the corresponding two-scale relation associated

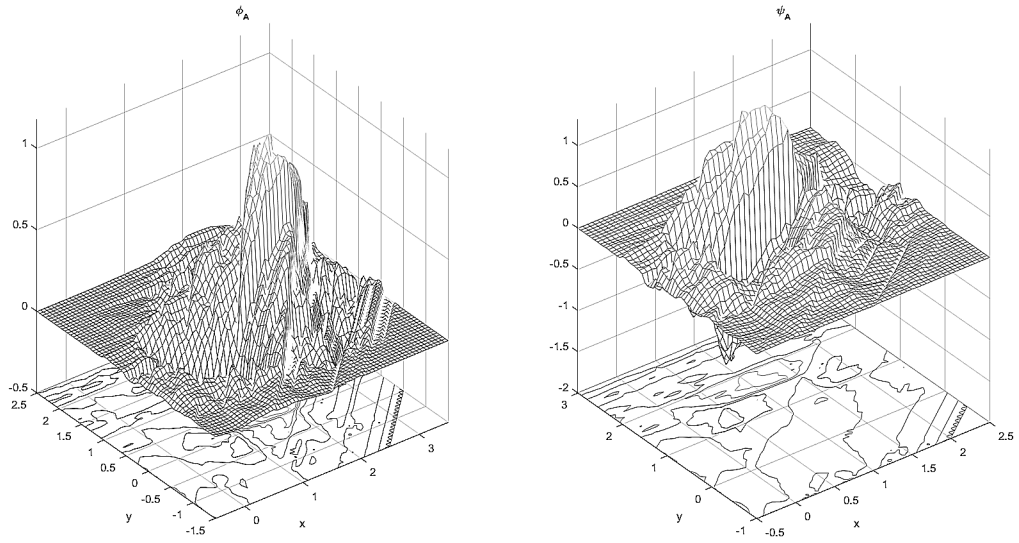

Figure 12: "Devil's Tower" Graphs before U_s

with A *and* $\{h_{\vec{n}}, \vec{n} \in \Lambda_0\}$,

$$\varphi_A = \sum_{\vec{n}\in\Lambda_0} h_{\vec{n}} D_A T_{\vec{n}} \varphi_A.$$

So we obtain the scaling function φ_A *as well as the Parseval's frame wavelet function* ψ_A *that associated with* A*. The graphs of* φ_A *and* ψ_A *are illustrated in Figure (12).*

$\psi_{A_0} \equiv U_S \psi_A$ *and* $\varphi_{A_0} \equiv U_S \varphi_A$ *are the wavelet and scaling function associated with matrix* A_0*. The graphs of* φ_{A_0} *and* ψ_{A_0} *are illustrated in Figure (13). This* φ_{A_0} *is known as the scaling function "Devil's Tower" (Fig. 5.1) in [4].*

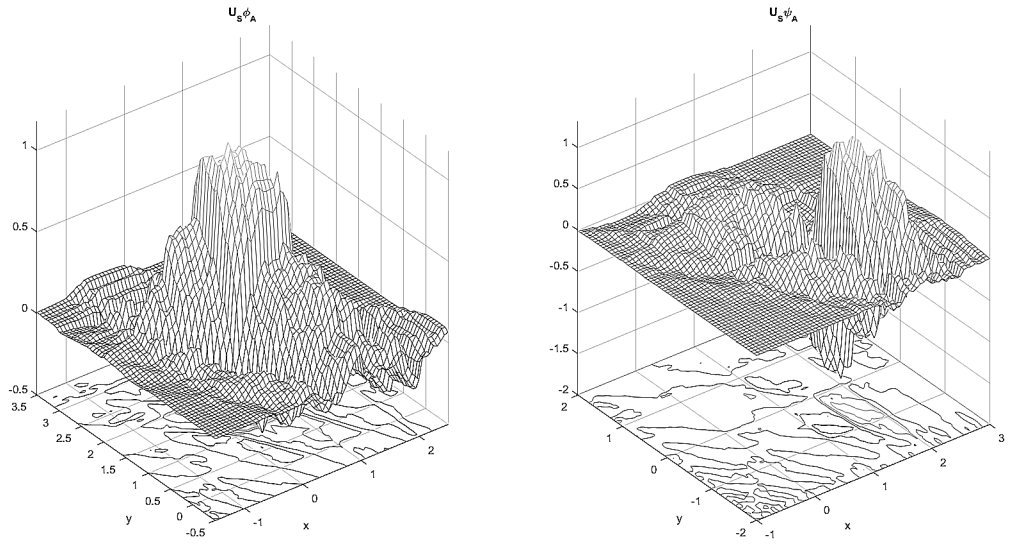

Figure 13: "Devil's Tower"Graphs

Example 2.3.4. *"Devil's Tower" variant*

Let

$$A = \begin{bmatrix} 1 & 1 \\ 1 & -1 \end{bmatrix}, S = \begin{bmatrix} 0 & 1 \\ 1 & -1 \end{bmatrix} \text{ and } A_0 = \begin{bmatrix} 0 & 2 \\ 1 & 0 \end{bmatrix}.$$

Then

$$A_0 = S^{-1}AS$$

We will construct the scaling function φ_A and the related Parseval's frame wavelet ψ_A associated with matrix A. Then, $U_S\varphi_A$ and $U_S\psi_A$ will be the scaling function and Parseval's frame wavelet associated with matrix A_0.

Assume that the support of solution is Λ_0, a 2×6 region:

$$\Lambda_0 = \left\{ \begin{bmatrix} 0 \\ m \end{bmatrix}, m = 0, 1, \cdots, 5 \right\} \cup \left\{ \begin{bmatrix} 1 \\ m \end{bmatrix}, m = -1, 0, \cdots, 5 \right\}$$

The reduced Lawton's system of equations related to Λ_0 associated with matrix A has

the following 10 *equations.*

$$\begin{cases} \sum_{n=0}^{5} h_{0,n} + h_{1,n} & = & \sqrt{2}, \\ \sum_{n=0}^{5} h_{0,n}^2 + h_{1,n}^2 & = & 1, \\ \sum_{n=0}^{3} h_{0,n} \cdot h_{0,n+2} + h_{1,n} \cdot h_{1,n+2} & = & 0, \\ \sum_{n=0}^{1} h_{0,n} \cdot h_{0,n+4} + h_{1,n} \cdot h_{1,n+4} & = & 0, \\ \sum_{n=0}^{0} h_{1,n} \cdot h_{0,n+5} & = & 0, \\ \sum_{n=0}^{2} h_{1,n} \cdot h_{0,n+3} & = & 0, \\ \sum_{n=0}^{4} h_{1,n} \cdot h_{0,n+5} & = & 0, \\ \sum_{n=0}^{4} h_{0,n} \cdot h_{1,n+1} & = & 0, \\ \sum_{n=0}^{2} h_{0,n} \cdot h_{1,n+3} & = & 0, \\ \sum_{n=0}^{0} h_{0,n} \cdot h_{1,n+5} & = & 0. \end{cases} \tag{28}$$

Table 3 is a solution to equation system (28)*. Note that this solution is basically the transpose of the previous solution.*

$h_{0,0}$	$h_{1,0}$	0	0.0473671727453765
$h_{0,1}$	$h_{1,1}$	-0.176776695296637	0.0473671727453765
$h_{0,2}$	$h_{1,2}$	0.176776695296637	0.659739608441171
$h_{0,3}$	$h_{1,3}$	0.176776695296637	0.659739608441171
$h_{0,4}$	$h_{1,4}$	-0.176776695296637	0
$h_{0,5}$	$h_{1,5}$	0	0

Table 3: A solution to Equations (28)

Based on this solution, we obtain the corresponding two-scale relation associated with A *and* $\{h_{\vec{n}}, \vec{n} \in \Lambda_0\}$,

$$\varphi_A = \sum_{\vec{n} \in \Lambda_0} h_{\vec{n}} D_A T_{\vec{n}} \varphi_A.$$

So we obtain the scaling function φ_A *as well as the Parseval's frame wavelet func-*

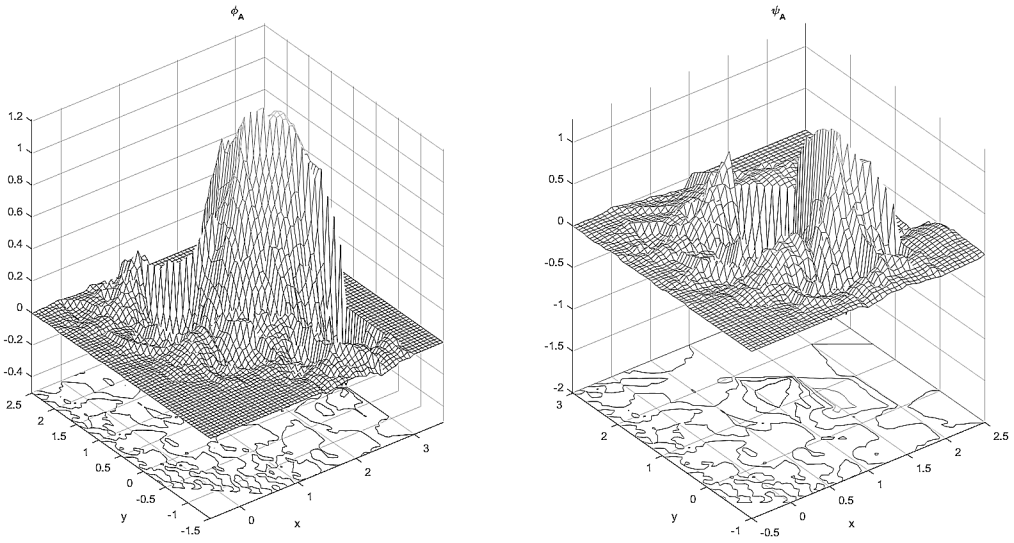

Figure 14: "Devil's Tower" variant Graphs before U_s

tion ψ_A that associated with A. The graphs of φ_A and ψ_A are illustrated in Figure (14).

If we apply the unitary operator U_S where $S = \begin{bmatrix} 0 & 1 \\ 1 & -1 \end{bmatrix}$, *we obtain the wavelet and scaling function associated with matrix* $A_0 = \begin{bmatrix} 0 & 2 \\ 1 & 0 \end{bmatrix}$. *The graphs of φ_{A_0} and ψ_{A_0} are illustrated in Figure (15). We haven't seen any graphs in the literature that resembles Figure (14) or Figure (15).*

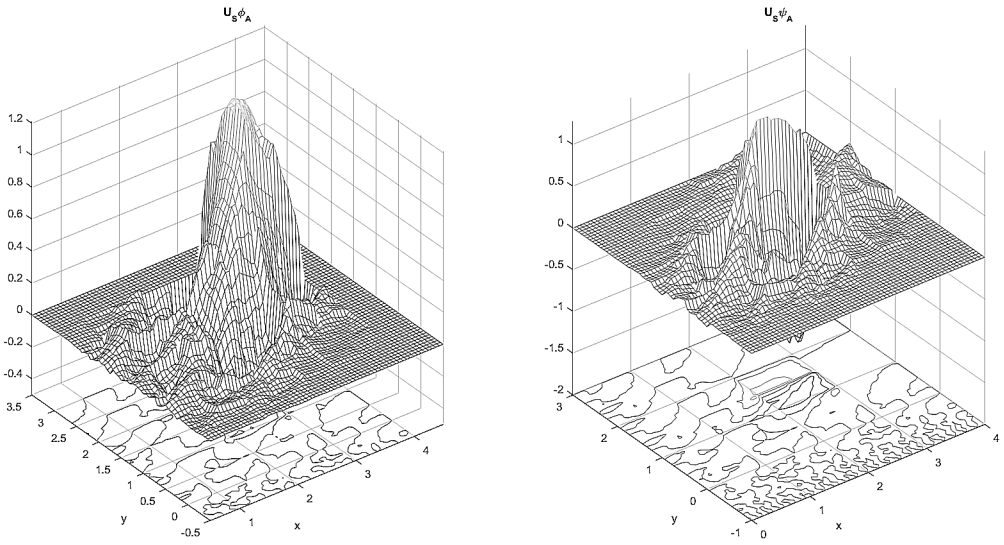

Figure 15: "Devil's Tower" variant Graphs

In the following 4 examples, we will focus on plotting the scaling function φ_A and wavelet function ψ_A, given the matrix

$$A = \begin{bmatrix} 1 & 1 \\ 1 & -1 \end{bmatrix}.$$

Note that, the Lawton's system of equations is solely determined by the given matrix A:

$$\begin{cases} \sum_{\vec{n}\in\mathbb{Z}^2} h_{\vec{n}}\overline{h_{\vec{n}+\vec{k}}} = \delta_{\vec{0}\vec{k}} \ ; \ \vec{k} \in A\mathbb{Z}^2 \\ \sum_{\vec{n}\in\mathbb{Z}^2} h_{\vec{n}} = \sqrt{2}. \end{cases} \tag{29}$$

Once we determined the support of solution: Λ_0, we can obtain infinitely number of numerical solutions to the Lawton's system of equations, since the system is under-determined.

The following examples will only list the numerical solutions and the graphs of scaling function φ_A and wavelet function ψ_A. We choose the support of solution Λ_0

to a 10×2 region, that is

$$\Lambda_0 = \left\{ \begin{bmatrix} 0 \\ \\ m \end{bmatrix}, m = 0, 1, \cdots, 9 \right\} \cup \left\{ \begin{bmatrix} 1 \\ \\ m \end{bmatrix}, m = 0, 1, \cdots, 9 \right\}$$

Some of the terms are zeroes in the numerical solutions, which indicates a reduced support.

Example 2.3.5. *Solution (a)*

$h_{0,0}$	$h_{0,1}$	0	0
$h_{1,0}$	$h_{1,1}$	0	0
$h_{2,0}$	$h_{2,1}$	0	0.557169520516259
$h_{3,0}$	$h_{3,1}$	0.0329212028753943	0.749763637537404
$h_{4,0}$	$h_{4,1}$	0.0443009172452429	0.249919657900581
$h_{5,0}$	$h_{5,1}$	-0.132903578450203	-0.185722018231522
$h_{6,0}$	$h_{6,1}$	0.0987642229799393	0
$h_{7,0}$	$h_{7,1}$	0	0
$h_{8,0}$	$h_{8,1}$	0	0
$h_{9,0}$	$h_{9,1}$	0	0

Table 4: Solution (a) to System (29) with Λ_0 size 10×2

The graphs of φ_A and ψ_A for Solution (a) is illustrated in Figure (16).

If we apply the unitary operator U_S where $S = \begin{bmatrix} 1 & 1 \\ \\ 1 & 0 \end{bmatrix}$, we obtain the wavelet and scaling function associated with matrix $A_0 = \begin{bmatrix} 0 & 1 \\ \\ 2 & 0 \end{bmatrix}$. We haven't seen any graphs in the literature that resembles Figure (16) or Figure (17).

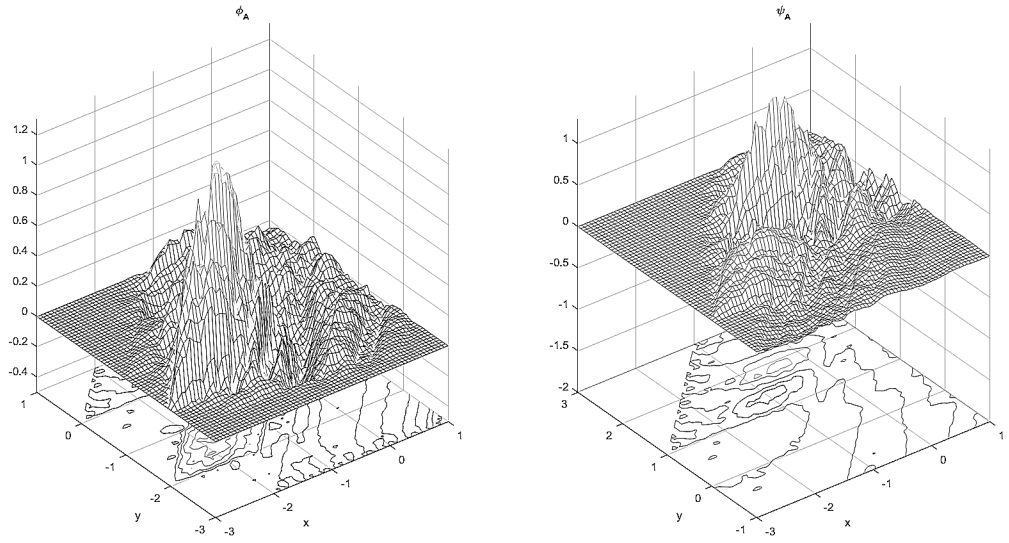

Figure 16: Function Graphs for Solution (a)

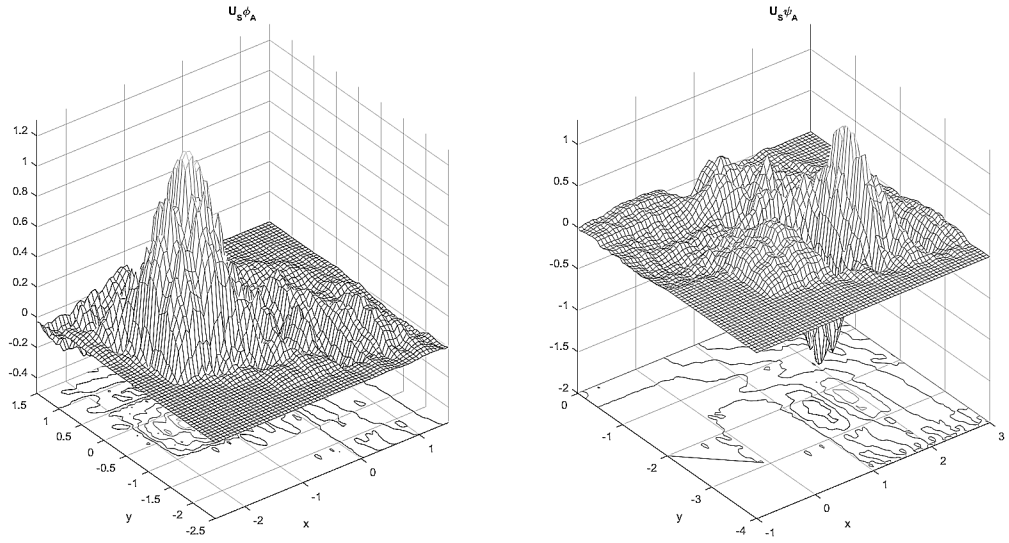

Figure 17: Function Graphs for Solution (a) after applying U_S

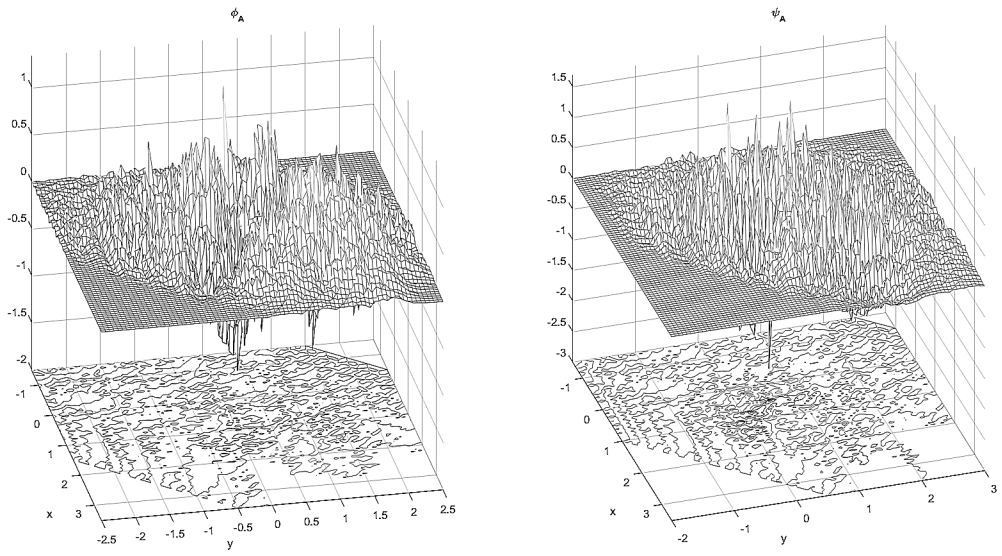

Figure 18: Function Graphs for Solution (b)

Example 2.3.6. *Solution (b) graphs in Figure (18)*

$h_{0,0}$	$h_{0,1}$	0	0
$h_{1,0}$	$h_{1,1}$	0	0
$h_{2,0}$	$h_{2,1}$	0	0.167399394135679
$h_{3,0}$	$h_{3,1}$	-0.296808460615992	-0.289943097871612
$h_{4,0}$	$h_{4,1}$	0.514085280832949	0.257372203040146
$h_{5,0}$	$h_{5,1}$	0.579143657062491	0.14859450413738
$h_{6,0}$	$h_{6,1}$	0.334370081652062	0
$h_{7,0}$	$h_{7,1}$	0	0
$h_{8,0}$	$h_{8,1}$	0	0
$h_{9,0}$	$h_{9,1}$	0	0

Table 5: Solution (b) to System (29) with Λ_0 size 10×2

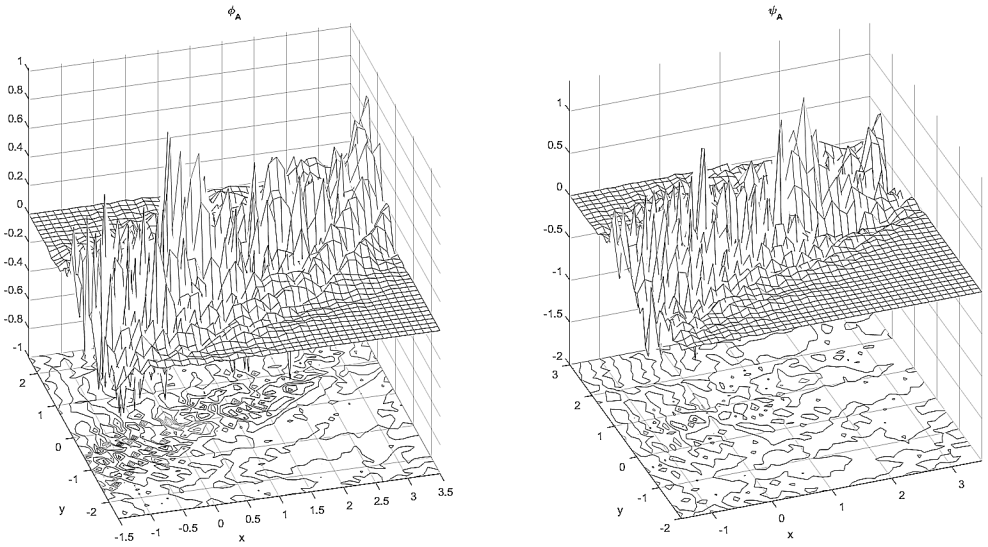

Figure 19: Function Graphs for Solution (c)

Example 2.3.7. *Solution (c) graphs in Figure (19)*

$h_{0,0}$	$h_{0,1}$	0	-0.042662356611308
$h_{1,0}$	$h_{1,1}$	0.229718118426660	0.073893369221408
$h_{2,0}$	$h_{2,1}$	-0.397883452534099	-0.058652899137267
$h_{3,0}$	$h_{3,1}$	-0.254614013976788	0.103058936292361
$h_{4,0}$	$h_{4,1}$	0.433086698471935	0.351421084047414
$h_{5,0}$	$h_{5,1}$	0.087682680580658	0.197167971333346
$h_{6,0}$	$h_{6,1}$	0.051683876078416	0.498309235953705
$h_{7,0}$	$h_{7,1}$	-0.092366711526760	0.287698971517548
$h_{8,0}$	$h_{8,1}$	-0.053327945764135	0
$h_{9,0}$	$h_{9,1}$	0	0

Table 6: Solution (c) to System (29) with Λ_0 size 10×2

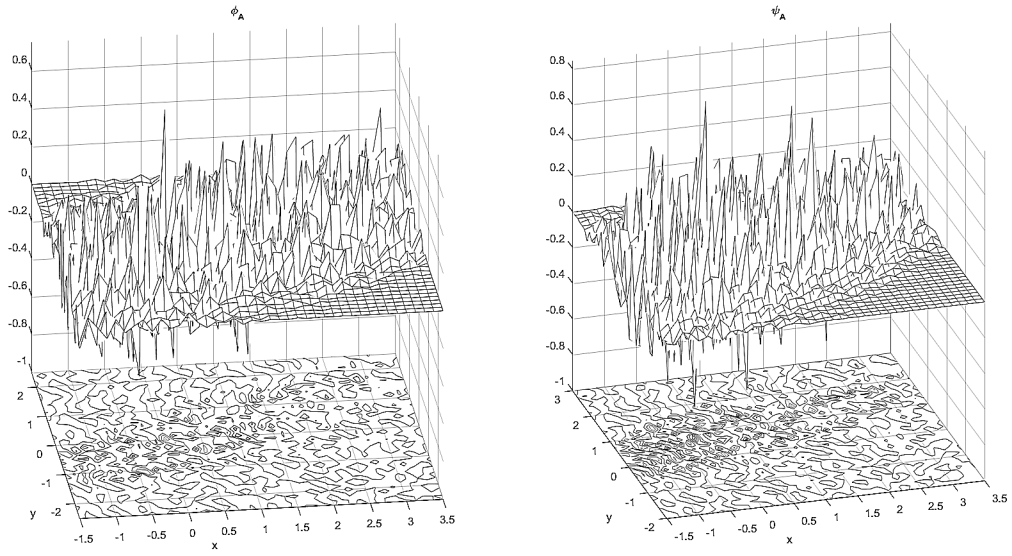

Figure 20: Function Graphs for Solution (d)

Example 2.3.8. *Solution (d) graphs in Figure (20)*

$h_{0,0}$	$h_{0,1}$	0	-0.071588157760280
$h_{1,0}$	$h_{1,1}$	0.156832894292099	0.123994326461062
$h_{2,0}$	$h_{2,1}$	-0.271642541211995	0.072824192521115
$h_{3,0}$	$h_{3,1}$	-0.372775372167982	-0.018099348797588
$h_{4,0}$	$h_{4,1}$	0.408980684972816	0.51321661540415
$h_{5,0}$	$h_{5,1}$	0.239130536943095	0.12516496091656
$h_{6,0}$	$h_{6,1}$	0.216030240651394	0.340205118613902
$h_{7,0}$	$h_{7,1}$	-0.154992908076327	0.196417516811425
$h_{8,0}$	$h_{8,1}$	-0.089485197200350	0
$h_{9,0}$	$h_{9,1}$	0	0

Table 7: Solution (d) to System (29) with Λ_0 size 10×2

2.4 Examples in $\mathrm{L}^2(\mathbb{R}^3)$

Example 2.4.1. *A Haar wavelet in $L^2(\mathbb{R}^3)$ associated with matrix*

$$A_0 \equiv \begin{bmatrix} 0 & 1 & 0 \\ 0 & 0 & 1 \\ 2 & 0 & 0 \end{bmatrix}.$$

We have $A_0 = S^{-1}AS$ where

$$A \equiv \begin{bmatrix} 0 & 2 & -1 \\ 0 & 0 & 1 \\ 1 & 1 & 0 \end{bmatrix} \text{ and } S \equiv \begin{bmatrix} -1 & 0 & 1 \\ 1 & 0 & 0 \\ 0 & 1 & 0 \end{bmatrix}.$$

Then $\det(A) = 2$ *with eigenvalues* $\{\sqrt[3]{2}e^{\frac{ik\pi}{3}}, k = 0, 1, 2.\}$. *The matrix A is expansive.*

We have

$$A\mathbb{Z}^3 = \left\{\alpha \begin{bmatrix} 0 \\ 0 \\ 1 \end{bmatrix} + \beta \begin{bmatrix} 1 \\ 1 \\ 0 \end{bmatrix} + (2\mathbb{Z})^3, \alpha, \beta \in \mathbb{Z}\right\} = A^{\intercal}\mathbb{Z}^3.$$

Let

$$\vec{\ell}_A \equiv \begin{bmatrix} 1 \\ 0 \\ 0 \end{bmatrix}, \ \vec{q}_A \equiv \begin{bmatrix} 1 \\ 1 \\ 0 \end{bmatrix}.$$

The vectors $\vec{\ell}_A, \vec{q}_A$ and matrix A satisfies the properties (1)-(5) in the Partition Theorem (Theorem 2.1). In this example we assume that the only non zero elements for

$h_{\vec{n}}$ *are at*

$$\vec{n}_0 = \begin{bmatrix} 0 \\ 0 \\ 0 \end{bmatrix} \text{ and } \vec{n}_1 = \begin{bmatrix} 1 \\ 0 \\ 0 \end{bmatrix} \in \vec{\ell}_A + A\mathbb{Z}^3.$$

So the product $h_{\vec{n}_0}\overline{h}_{\vec{n}_1}$ *is not in any of the equations. The reduced Lawton's System of Equations is*

$$\begin{cases} h_{\vec{n}_0}^2 + h_{\vec{n}_1}^2 = 1 \\ h_{\vec{n}_0} + h_{\vec{n}_1} = \sqrt{2}. \end{cases}$$

The system has one solution $h_{\vec{n}_0} = h_{\vec{n}_1} = \frac{\sqrt{2}}{2}$.

The two-scale relation equation (22) *is*

$$\varphi_A = \frac{\sqrt{2}}{2} D_A (I + T_{\vec{n}_1})\varphi_A.$$

By Step 5 in Theorem 2.1,

$$\varphi_{A_0} = U_S \varphi_A = \frac{\sqrt{2}}{2} D_{A_0}(I + T_{S^{-1}\vec{n}_1})\varphi_{A_0} = \frac{\sqrt{2}}{2} D_{A_0}(I + T_{\vec{e}_3})\varphi_{A_0}.$$

Notice that we have $(I + T_{\vec{e}_3})\chi_{[0,1)^3} = \chi_{[0,1)^2\times[0,2)}$ *and* $\frac{\sqrt{2}}{2} D_{A_0}\chi_{[0,1)^2\times[0,2)} = \chi_{[0,1)^3}$. *The function* $\chi_{[0,1)^3}$ *is the scaling function* φ_{A_0}. *Then the related normalized tight frame (orthogonal) wavelet is*

$$\psi_{A_0} = \chi_{Q^+} - \chi_{Q^-}, \text{ with } Q^+ \equiv \chi_{[0,0.5)\times[0,1)^2} \text{ and } Q^- \equiv \chi_{[0.5,1)\times[0,1)^2}$$

This is a Haar wavelet in $L^2(\mathbb{R}^3)$.

The function graphs of φ_A, ψ_A, *and the resulting functions after applied* U_S, φ_{A_0} *and* ψ_{A_0}, *are in illustrated in Figure (21) and Figure (22).*

With this method, we can find examples of Haar wavelets in any dimension.

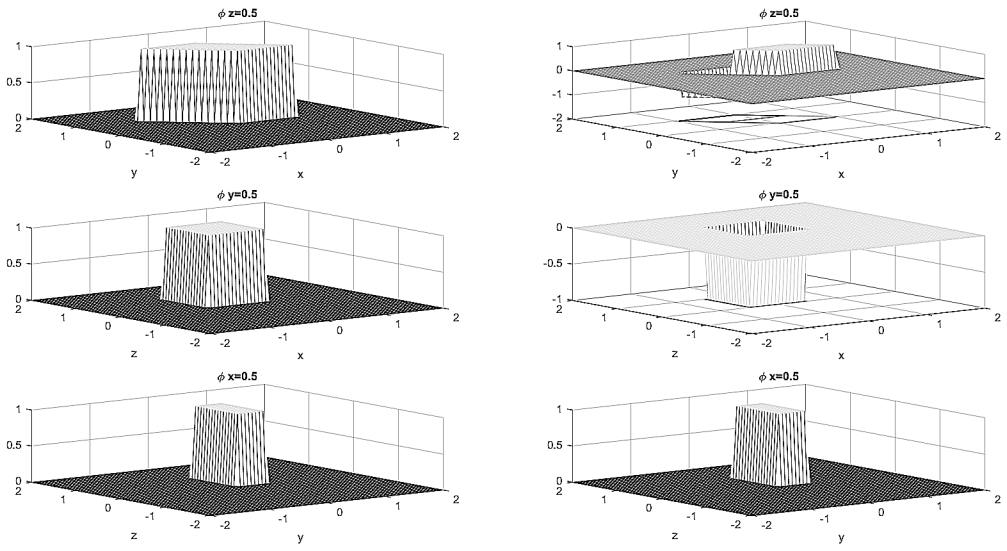

Figure 21: Function Graphs for A Haar wavelet in $L^2(\mathbb{R}^3)$ before U_S

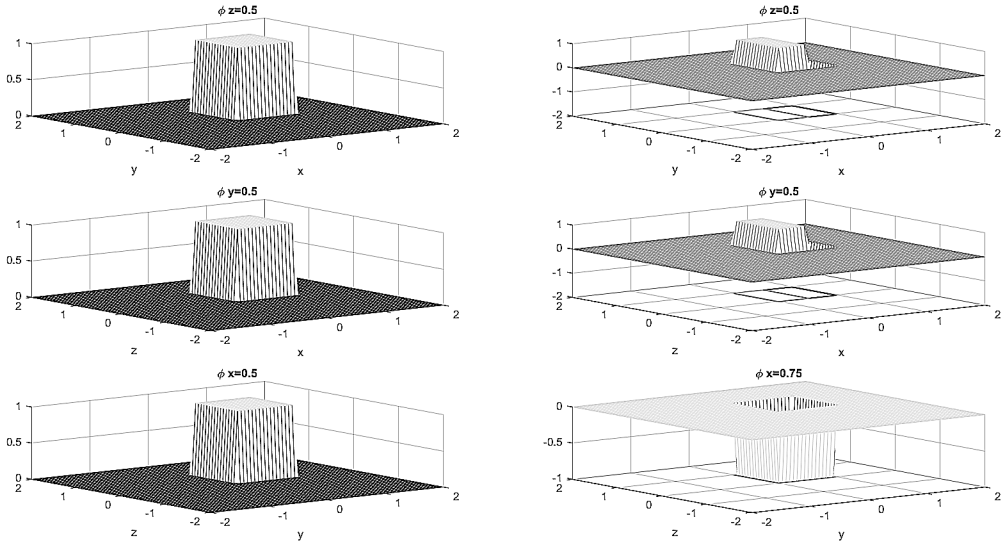

Figure 22: Function Graphs for A Haar wavelet in $L^2(\mathbb{R}^3)$

Example 2.4.2. *Let*

$$A \equiv \begin{bmatrix} -2 & 1 & -2 \\ 1 & 0 & 0 \\ 2 & 0 & 2 \end{bmatrix}, \vec{\ell}_A \equiv \begin{bmatrix} 0 \\ 0 \\ 1 \end{bmatrix} \text{ and } \vec{q}_A \equiv \begin{bmatrix} 0 \\ 0 \\ 1 \end{bmatrix}.$$

It is clear that $\det(A) = -2$. *Also, we have*

$$A\mathbb{Z}^3 = \left\{\alpha\vec{e}_1 + \beta\vec{e}_2 + (2\mathbb{Z})^3, \alpha, \beta \in \mathbb{Z}\right\} = A^\tau\mathbb{Z}^3.$$

The vectors $\vec{\ell}_A, \vec{q}_A$ *and matrix* A *satisfy the properties (1)-(5) in the Partition Theorem (Theorem 2.1). So, given a finite solution to the Lawton's System of Equations, we will have a Parseval's frame wavelet associated with matrix* A.

In this example we choose

$$\Lambda_0 \equiv \left\{\vec{n} = \alpha\vec{e}_1 + \beta\vec{e}_2 + \gamma\vec{e}_3,\ \alpha = 0, 1, 2, 3,\ \beta = 0, 1,\ \gamma = 0, 1, \right\}.$$

The corresponding reduced Lawton's system of equations is

$$
\begin{cases}
\sum_{\vec{n}\in\Lambda_0} h_{\vec{n}}^2 & = \quad 1, \\
\sum_{\vec{n}\in\Lambda_0} h_{\vec{n}} & = \quad \sqrt{2}, \\
\sum_{k=0}^{3}(h_{k,0,0}\cdot h_{(1+k),0,0} + h_{k,0,1}\cdot h_{(1+k),0,1} + h_{k,1,0}\cdot h_{(1+k),1,0} + h_{k,1,1}\cdot h_{(1+k),1,1}) & = \quad 0, \\
\sum_{k=0}^{2}(h_{k,0,0}\cdot h_{(2+k),0,0} + h_{k,0,1}\cdot h_{(2+k),0,1} + h_{k,1,0}\cdot h_{(2+k),1,0} + h_{k,1,1}\cdot h_{(2+k),1,1}) & = \quad 0, \\
\sum_{k=0}^{1}(h_{k,0,0}\cdot h_{(3+k),0,0} + h_{k,0,1}\cdot h_{(3+k),0,1} + h_{k,1,0}\cdot h_{(3+k),1,0} + h_{k,1,1}\cdot h_{(3+k),1,1}) & = \quad 0, \\
\sum_{k=0}^{0}(h_{k,0,0}\cdot h_{(3+k),1,0} + h_{k,0,1}\cdot h_{(3+k),1,1}) & = \quad 0, \\
\sum_{k=0}^{1}(h_{k,0,0}\cdot h_{(2+k),1,0} + h_{k,0,1}\cdot h_{(2+k),1,1}) & = \quad 0, \\
\sum_{k=0}^{2}(h_{k,0,0}\cdot h_{(1+k),1,0} + h_{k,0,1}\cdot h_{(1+k),1,1}) & = \quad 0, \\
\sum_{k=0}^{3}(h_{k,0,0}\cdot h_{k,1,0} + h_{k,0,1}\cdot h_{k,1,1}) & = \quad 0, \\
\sum_{k=1}^{3}(h_{k,0,0}\cdot h_{(k-1),1,0} + h_{k,0,1}\cdot h_{(k-1),1,1}) & = \quad 0, \\
\sum_{k=2}^{3}(h_{k,0,0}\cdot h_{(k-2),1,0} + h_{k,0,1}\cdot h_{(k-2),1,1}) & = \quad 0, \\
\sum_{k=3}^{3}(h_{k,0,0}\cdot h_{(k-3),1,0} + h_{k,0,1}\cdot h_{(k-3),1,1}) & = \quad 0
\end{cases}
\tag{30}
$$

Solutions to this system of equations (30) *are plentiful. In Table 8 we show two sets of solutions. The solution satisfies the equations* (30) *within errors less than* 10^{-13}.

α	β	γ	Solution (1)	Solution (2)
0	0	0	0.00000000000000003754	-0.00000000000000000294
1	0	0	0.08378339374280850000	0.03292120287539430000
2	0	0	0.49453510790101500000	-0.13290357845020300000
3	0	0	0.00000000000000024969	0.00000000000000017890
0	1	0	0.00000000000000002218	0.00000000000000004947
1	1	0	0.35330635188230000000	0.55716952051625900000
2	1	0	-0.22451807131547000000	0.24991965790058100000
3	1	0	0.00000000000000011746	-0.00000000000000000691
0	0	1	0.00000000000000007270	-0.00000000000000000396
1	0	1	0.16226597620431900000	0.04430091724524290000
2	0	1	-0.25534514772672400000	0.09876422297993930000
3	0	1	-0.00000000000000012892	-0.00000000000000013295
0	1	1	0.00000000000000004295	0.00000000000000006657
1	1	1	0.68425970262500800000	0.74976363753740400000
2	1	1	0.11592624905984000000	-0.18572201823152200000
3	1	1	-0.00000000000000006065	0.00000000000000000514

Table 8: Solutions to System (30) with Λ_0 size $4 \times 2 \times 2$

CHAPTER 3: ONE DIMENSION AND HIGH DIMENSION

In one dimension, plenty of wavelet coefficients have been proposed and studied. Here, we will illustrate an approach that will convert one dimension wavelet coefficients into high dimension ones.

In the 2D case, we use $A = \begin{bmatrix} -1 & 2 \\ -2 & 2 \end{bmatrix}$ as the default dilation matrix for this chapter. Recall that a dilation matrix is used to populated the Lawton's System of Equations for the wavelet coeffients.

We start with a well-known wavelet – db16, and its graphs are shown in Figure (23).

h_1	0.0544158422431072
h_2	0.3128715909143166
h_3	0.6756307362973795
h_4	0.5853546836542159
h_5	-0.0158291052563823
h_6	-0.2840155429615824
h_7	0.0004724845739124
h_8	0.1287474266204893
h_9	-0.0173693010018090
h_{10}	-0.0440882539307971
h_{11}	0.0139810279174001
h_{12}	0.0087460940474065
h_{13}	-0.0048703529934520
h_{14}	-0.0003917403733770
h_{15}	0.0006754494064506
h_{16}	-0.0001174767841248

Table 9: Wavelet Coefficients for db16

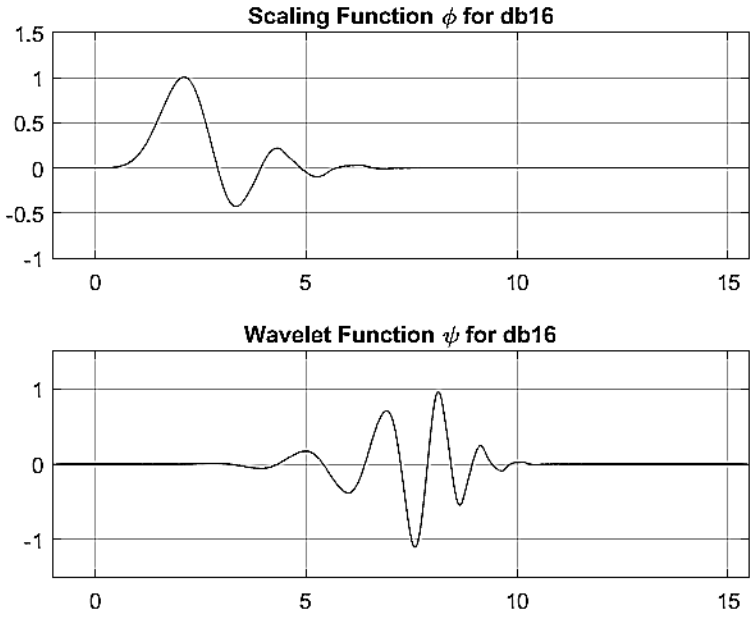

Figure 23: Graphs of db16

Its wavelet coefficients satisfy the following Lawton's System of Equations 31.

$$\begin{cases} \sum_{n=1}^{16} h_n & = & \sqrt{2}, \\ \sum_{n=1}^{16} h_n^2 & = & 1, \\ \sum_{n=1}^{14} h_n \cdot h_{n+2} & = & 0, \\ \sum_{n=1}^{12} h_n \cdot h_{n+4} & = & 0, \\ \sum_{n=1}^{10} h_n \cdot h_{n+6} & = & 0, \\ \sum_{n=1}^{8} h_n \cdot h_{n+8} & = & 0, \\ \sum_{n=1}^{6} h_n \cdot h_{n+10} & = & 0, \\ \sum_{n=1}^{4} h_n \cdot h_{n+12} & = & 0, \\ \sum_{n=1}^{2} h_n \cdot h_{n+14} & = & 0. \end{cases} \tag{31}$$

In the 2D case, given the support of the solution is 2×8, the associated Lawton's

System of Equations is:

$$\begin{cases} \sum_{n=1}^{8} h_{1,n} + h_{2,n} & = & \sqrt{2}, \\ \sum_{n=1}^{8} h_{1,n}^2 + h_{2,n}^2 & = & 1, \\ \sum_{n=1}^{7} h_{1,n} \cdot h_{1,n+1} + h_{2,n} \cdot h_{2,n+1} & = & 0, \\ \sum_{n=1}^{6} h_{1,n} \cdot h_{1,n+2} + h_{2,n} \cdot h_{2,n+2} & = & 0, \\ \sum_{n=1}^{5} h_{1,n} \cdot h_{1,n+3} + h_{2,n} \cdot h_{2,n+3} & = & 0, \\ \sum_{n=1}^{4} h_{1,n} \cdot h_{1,n+4} + h_{2,n} \cdot h_{2,n+4} & = & 0, \\ \sum_{n=1}^{3} h_{1,n} \cdot h_{1,n+5} + h_{2,n} \cdot h_{2,n+5} & = & 0, \\ \sum_{n=1}^{2} h_{1,n} \cdot h_{1,n+6} + h_{2,n} \cdot h_{2,n+6} & = & 0, \\ \sum_{n=1}^{1} h_{1,n} \cdot h_{1,n+7} + h_{2,n} \cdot h_{2,n+7} & = & 0. \end{cases} \tag{32}$$

The following set of wavelet coefficients is a valid solution to system (32):

$h_{1,1}$	$h_{2,1}$	0.0544158422431072	0.3128715909143166
$h_{1,2}$	$h_{2,2}$	0.6756307362973795	0.5853546836542159
$h_{1,3}$	$h_{2,3}$	-0.0158291052563823	-0.2840155429615824
$h_{1,4}$	$h_{2,4}$	0.0004724845739124	0.1287474266204893
$h_{1,5}$	$h_{2,5}$	-0.0173693010018090	-0.0440882539307971
$h_{1,6}$	$h_{2,6}$	0.0139810279174001	0.0087460940474065
$h_{1,7}$	$h_{2,7}$	-0.0048703529934520	-0.0003917403733770
$h_{1,8}$	$h_{2,8}$	0.0006754494064506	-0.0001174767841248

Table 10: Wavelet Coefficients for a $2D$ version of db16

Note that, all terms in the above solution are actually from db16, the one dimension solution. We only rearranged the terms as follows: $h_{1,1} = h_1$, $h_{2,1} = h_2$, $h_{1,2} = h_3$, $h_{2,2} = h_4$, ..., $h_{1,8} = h_{15}$, $h_{2,8} = h_{16}$. A close examination shows that the two systems of equations, (31) and (32), are the same after applying the above mentioned substitution.

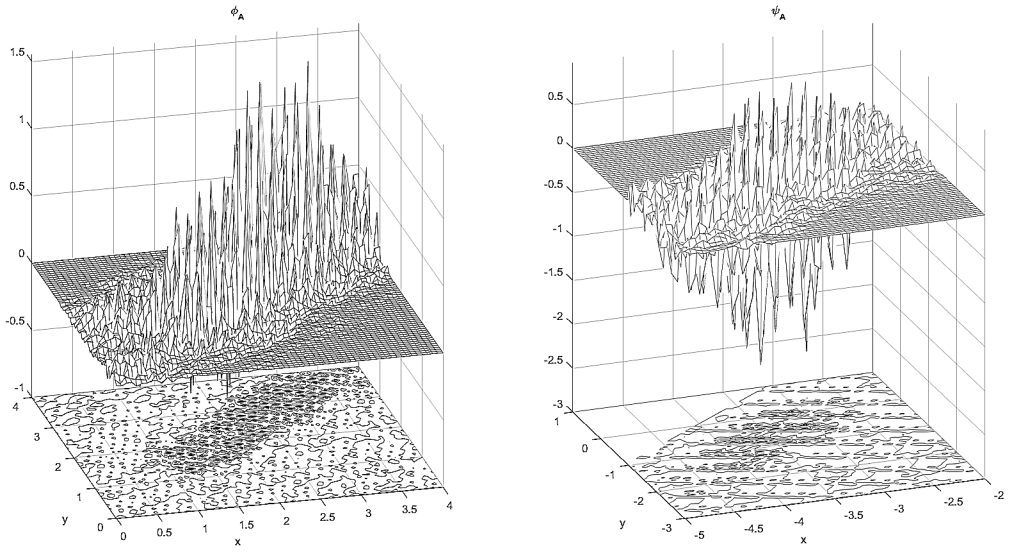

Figure 24: Graphs of a 2D version derived from db16

The graphs of the 2D scaling function and wavelet function are in Figure (24).

Following the above approach, we can construct other 2D wavelets from known 1D wavelet coefficients.

db8 is another well-known wavelet and its graph is shown in Figure (25).

h_1	0.2303778133088964
h_2	0.7148465705529154
h_3	0.6308807679298587
h_4	-0.0279837694168599
h_5	-0.1870348118790931
h_6	0.0308413818355607
h_7	0.0328830116668852
h_8	-0.0105974017850690

Table 11: Wavelet Coefficients for db8

The wavelet coefficients satisfy the following Lawton's System of Equations in 33:

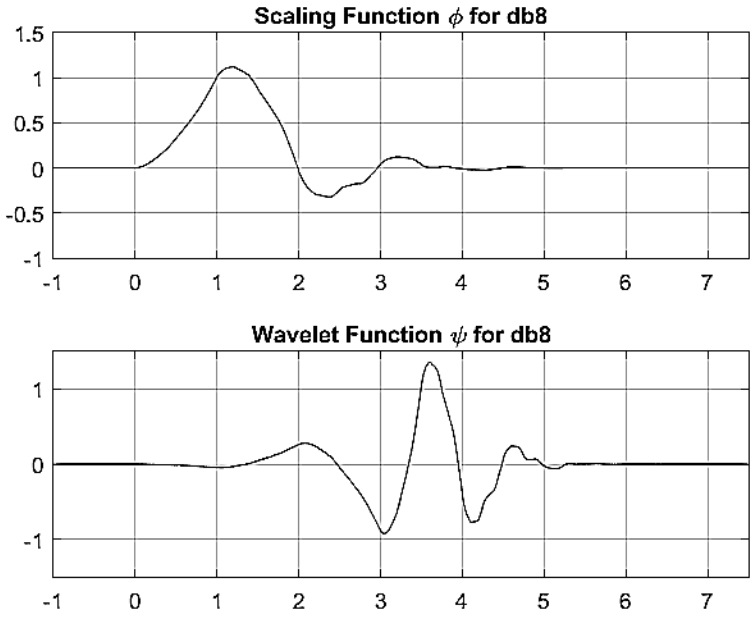

Figure 25: Graphs of db8

$$\begin{cases} \sum_{n=1}^{8} h_n & = & \sqrt{2}, \\ \sum_{n=1}^{8} h_n^2 & = & 1, \\ \sum_{n=1}^{6} h_n \cdot h_{n+2} & = & 0, \\ \sum_{n=1}^{4} h_n \cdot h_{n+4} & = & 0, \\ \sum_{n=1}^{2} h_n \cdot h_{n+6} & = & 0. \end{cases} \tag{33}$$

In the 2D case, given the support of the solution is 2×4, the associated Lawton's System of Equations is:

$$\begin{cases} \sum_{n=1}^{4} h_{1,n} + h_{2,n} & = & \sqrt{2}, \\ \sum_{n=1}^{4} h_{1,n}^2 + h_{2,n}^2 & = & 1, \\ \sum_{n=1}^{3} h_{1,n} \cdot h_{1,n+1} + h_{2,n} \cdot h_{2,n+1} & = & 0, \\ \sum_{n=1}^{2} h_{1,n} \cdot h_{1,n+2} + h_{2,n} \cdot h_{2,n+2} & = & 0, \\ \sum_{n=1}^{1} h_{1,n} \cdot h_{1,n+3} + h_{2,n} \cdot h_{2,n+3} & = & 0. \end{cases} \tag{34}$$

The following set of wavelet coefficients is a valid solution to system (34):

$h_{1,1}$	$h_{2,1}$	0.2303778133088964	0.7148465705529154
$h_{1,2}$	$h_{2,2}$	0.6308807679298587	-0.0279837694168599
$h_{1,3}$	$h_{2,3}$	-0.1870348118790931	0.0308413818355607
$h_{1,4}$	$h_{2,4}$	0.0328830116668852	-0.0105974017850690

Table 12: Wavelet Coefficients for a $2D$ version of db8

Note that, all terms in the above solution are actually from db8, the one dimension solution. We only rearranged the terms as follows: $h_{1,1} = h_1$, $h_{2,1} = h_2$, $h_{1,2} = h_3$, $h_{2,2} = h_4$, ..., $h_{1,4} = h_7$, $h_{2,4} = h_8$. A close examination shows that the two systems of equations, (33) and (34), are the same after applying the above mentioned substitution.

The graphs of the 2D scaling function and wavelet function are in Figure (26).

Lastly, we want to show that we can do the same to db4.

The wavelet coefficients for db4 are:

h_1	0.4829629131445341
h_2	0.8365163037378077
h_3	0.2241438680420134
h_4	-0.1294095225512603

Table 13: Wavelet Coefficients for db4

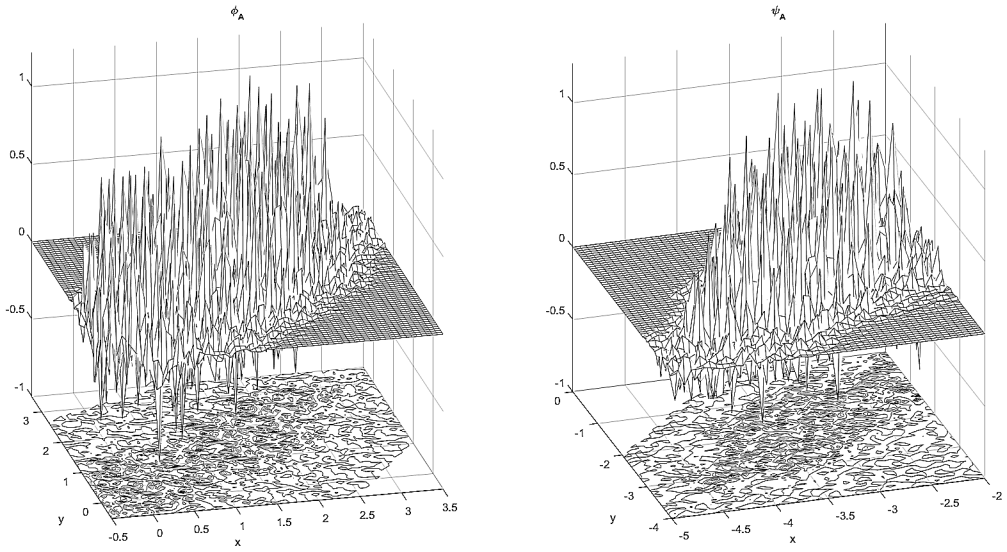

Figure 26: Graphs of a 2D version derived from db8

The Lawton's Systems of Equations for both 1D and 2D are listed below:

$$\text{1D}\begin{cases} \sum_{n=1}^{4} h_n = \sqrt{2}, \\ \sum_{n=1}^{4} h_n^2 = 1, \\ h_1 \cdot h_2 + h_3 \cdot h_4 = 0. \end{cases} \quad \text{2D}\begin{cases} \sum_{n=1}^{2} h_{1,n} + h_{2,n} = \sqrt{2}, \\ \sum_{n=1}^{2} h_{1,n}^2 + h_{2,n}^2 = 1, \\ h_{1,1} \cdot h_{2,1} + h_{1,2} \cdot h_{2,2} = 0. \end{cases}$$

The reader can find out the pattern of mapping from 1D terms into 2D terms.

The graphs for both 1D and 2D scaling functions and wavelet functions are shown in Figure (27) and Figure (28).

So given a set of wavelet coefficients in one dimension, we can obtain high dimension wavelet coefficients sets by rearranging the terms. As long as the new coefficients set satisfies the high dimension Lawton's System of Equations, the constructed scaling function and wavelet function from its 1D counterpart are valid 2D scaling function and wavelet function in 2D.

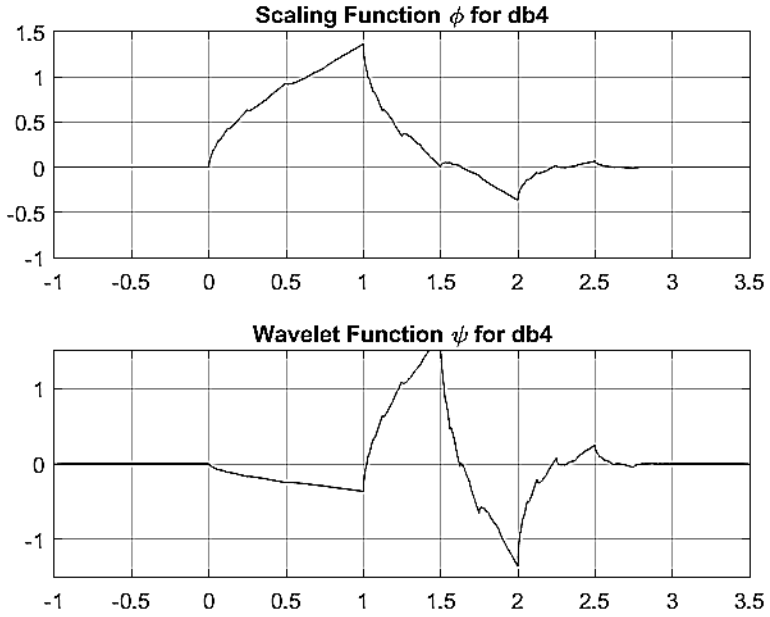

Figure 27: Graphs of db4

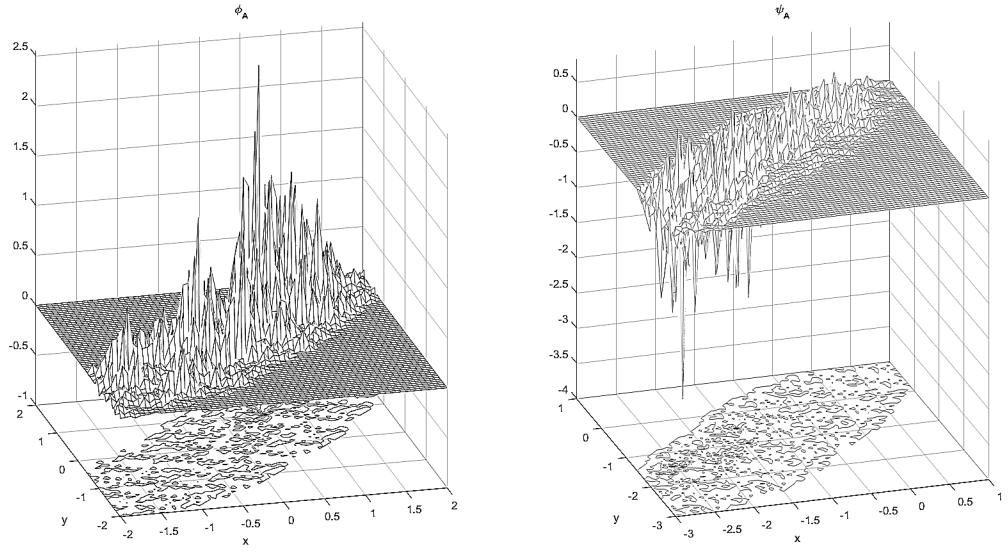

Figure 28: Graphs of a 2D version derived from db4

The above examples also show that, given a set of wavelet coefficients that satisfies the 2D Lawton's System of Equations, we can obtain an 1D version of the same set of numbers, which satisfies the 1D Lawton's System of Equations. And we can construct a 1D scaling function and wavelet function using the new 1D wavelet coefficients.

An interesting observation we have is that, while the smoothness of Daubechies' wavelet(db16, db8, db4 etc.) in 1D is decent, the smoothness is not carried over to the 2D counterparts. We would like to explore this further in the future, as there are many different ways to construct high dimension wavelet functions from 1D wavelet coefficients. We here only proposed one possible way that is associated with the given matrix A.

CHAPTER 4: APPLICATION OF FRAMES IN SIGNAL PROCESSING

In Section 1.3, we discussed a discrete wavelet transform(DWT) algorithm that can be used to decompose as well as perfectly reconstruct signals in one dimension. The theory behind the algorithm is captured completely by the orthogonal MRA framework.

In this chapter, we will demonstrate that this algorithm can be (1) implemented with frame MRA to decompose signals. That is, we can use frame wavelets and frame wavelets coefficients, rather than using the counterpart of orthogonal wavelets; (2) extend to higher dimensions with a different, more natural sub-lattice scheme.

Classically, the DWT is defined for signal sequences with length of powers of 2. Various methods can be used for extending signal samples of other sizes, including zero-padding, smooth padding, periodic extension, and boundary value replication (symmetrization). For simplicity of the presentation in the dissertation, we will omit the discussion of these methods and work only on examples with signal length of powers of 2.

4.1 Signal Analysis – 1-dimensional Case

In Section 2.1, we have already shown that, frame wavelets can be constructed from $\{h_n\}$, a solution to the Lawton's System of Equations. We call a even length $\{h_n\}$ **scaling filter**, denoted as H. As a matter of fact, Lawton's System of Equations gives a way to obtain the scaling filters.

In signal processing, a filter with finite impulse response(FIR)(or response to any finite length input) is called an **FIR filter**.

As discussed before, the fast cascading DWT algorithm is a classical two-channel subband scheme with quadrature mirror filters (QMFs). The direct connection between the solution of Lawton's System of Equations and QMFs is that we can derive all 4 QMFs from H, which is illustrated in the following chart:

Filter	Description	Note
Lo_R = norm(H)	Low-Pass Reconstruction Filter	normalize with sum $\sqrt{2}$
Hi_R = qmf(Lo_R)	High-Pass Reconstruction Filter	$Y(k) = (-1)^k X(N+1-k)$, N the length of the filter
Lo_D = rev(Lo_R)	Low-Pass Decomposition Filter	flips Lo_R
Hi_D = rev(Hi_R)	High-Pass Decomposition Filter	flips Hi_R

Table 14: Computing Quadrature Mirror Filters from Scaling Filter

Before we go deep dive into the details of the example of DWT, we need one more operation defined:

Definition 4.1. *Let S be a signal sequence and H a FIR filter with length N, then the discrete convolution between S and H is*

$$(S * H)(n) = \sum_{m=1}^{m=N} S(n-m)H(m).$$

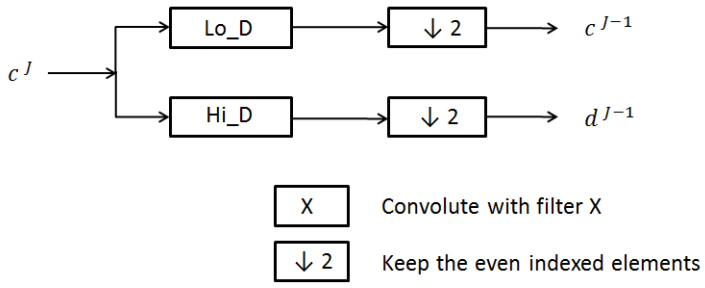

Figure 29: Decomposition from c^j to c^{j-1} and d^{j-1}

Note that S can be zero-padded and the length of the resulting sequence equals the length of S plus $N-1$.

Recall the decomposition formulas we have in Section 1.3:

$$\begin{cases} c_k^{j-1} = \sum_n \overline{h_{n-2k}} c_n^j; \\ d_k^{j-1} = \sum_n \overline{g_{n-2k}} c_n^j. \end{cases}$$

In practice, we do the following to obtain c^{j-1} from c^j:

Step 1. Convolute c^{j-1} with Lo_D;

Step 2. Downsample(dyadic decimation) the result from last step, this is c^{j-1}.

Some algebra exercises will show that this practical approach is equivalent to the decomposition formula.

Similarly, we have the following to obtain d^{j-1} from c^j:

Step 1. Convolute c^{j-1} with Hi_D;

Step 2. Downsample(dyadic decimation) the result from last step, this is d^{j-1}.

Notice that, the only difference between the two is the filter used in Step 1. We illustrate this decomposition process in Figure (29).

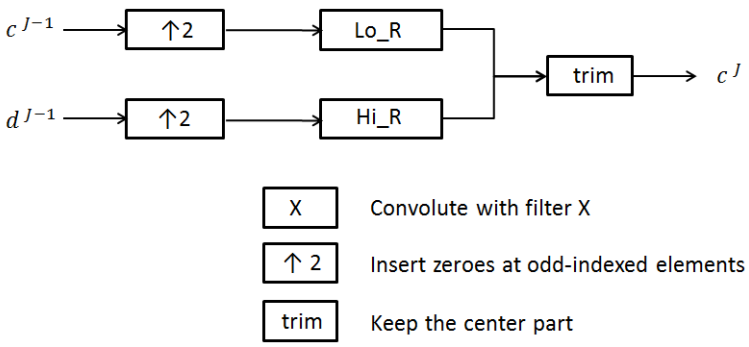

Figure 30: Reconstruction from c^{j-1} and d^{j-1} to c^j

For the reconstruction, recall the formula is:

$$c_n^j = \sum_k \left[h_{n-2k} c_k^{j-1} + g_{n-2k} d_k^{j-1} \right].$$

And in practice, we use the following approach which leads to the same c^j as in the reconstruction formula.

Step 1. Upsample(dyadic zero inserting) c^{j-1};

Step 2. Convolute the result from last step with Lo_R, this is the first summation in the reconstruction formula;

Step 3. Upsample(dyadic zero inserting) d^{j-1};

Step 4. Convolute the result from last step with Hi_R, this is the second summation in the reconstruction formula;

Step 5. Add the results from Step 2 and Step 4. The center part of the sum is c^j.

This reconstruction process is illustrated in Figure (30).

Example 4.1.1. *2-level decomposition and reconstruction with orthogonal wavelet "db4".*

The original signal is of length 128. *We first decomposed it into cA*1 *and cD*1. *Then further decomposed cA*1 *into cA*2 *and cD*2. *On the reconstruction part, we*

started from cA2, cD2 and cD1, and first reconstructed cA1 from cA2 and cD2, and then reconstructed the original signal from the reconstructed cA1 and cD1.

The following is the Matlab script for the process.

```
% Load data
load leleccum;
S = leleccum(1:128);


% db4 wavelet coefficient
H = [0.34150635094622   0.591506350945867
     0.158493649053779 -0.091506350945867]*sqrt(2);


% Compute the 4 QMFs w.r.t H
[Lo_D,Hi_D,Lo_R,Hi_R] = orthfilt(H);


% Decomposition Level 1
% Convolution with Lo_D and downsampling to get Appr. Coef. -- cA1
% downsampling, retaining even-indexed terms
cA1 = dyaddown( conv(Lo_D,S) ,0);
% Convolution with Hi_D and downsampling to get Detail Coef. -- cD1
% downsampling, retaining even-indexed terms
cD1 = dyaddown( conv(Hi_D,S) ,0);
```

```
% Decomposition Level 2

% Convolution with Lo_D and downsampling to get Appr. Coef. -- cA2

% downsampling, retaining even-indexed terms

cA2 = dyaddown( conv(Lo_D,cA1) ,0);

% Convolution with Hi_D and downsampling to get Detail Coef. -- cD2

% downsampling, retaining even-indexed terms

cD2 = dyaddown( conv(Hi_D,cA1) ,0);


% Here we have the approximation cA2 and the details sequence cD2, cD1


% Reconstrucion Level 2

% Reconstruct cA1 from cA2 and cD2

% pad zeros at odd-index of cA2 and cD2

% conv with Lo_R and Hi_R respectively

cA1_r = conv(Lo_R,dyadup(cA2,1)) + conv(Hi_R,dyadup(cD2,1));

% keep the central part of cA1_r with the same length as cA1

cA1_r_trim = wkeep(cA1_r,length(cA1),'c');


% Reconstrucion Level 1

% Reconstruct SS from cA1_r_trim and cD1

% pad zeros at odd-index of cA1_r_trim and cD1,

% conv with Lo_R and Hi_R respectively

S_r = conv(Lo_R,dyadup(cA1_r_trim,1)) + conv(Hi_R,dyadup(cD1,1));
```

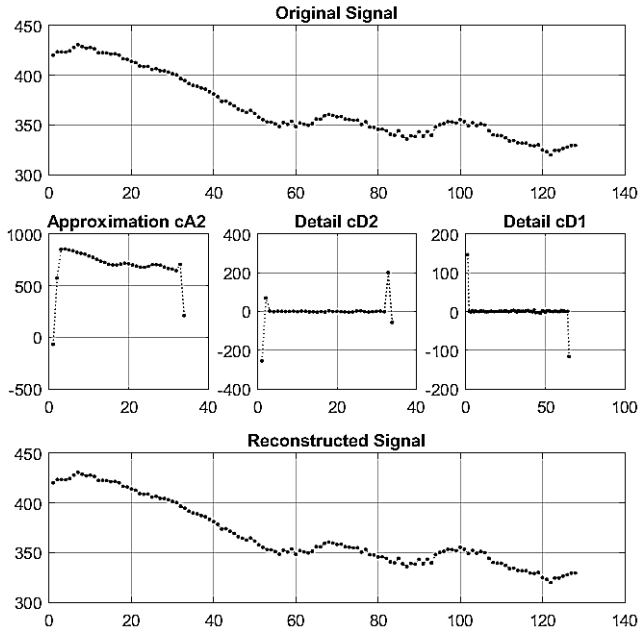

Figure 31: 2-level Signal Analysis Example

```
% keep the central part of S_r with the same length as original signal S

S_r_trim = wkeep(S_r,length(S),'c');


% S_r_trim is the reconstructed signal
```

4.2 Image Decomposition – 2-dimensional Case

The traditional approach when applying DWT in a 2D scenario is to use tensor product. That is, to apply the 1D DWT algorithm to x-axis and y-axis respectively. The details of this approach can be found in [8].

Here in this section, we propose a different approach that utilizes the so called quincunx sub-lattice in 2D. This is a natural 2D extension than the traditional method because here we are working on both axes simultaneously.

The work flow resembles the 1D case, only that we are applying a 2D convolution.

Given matrix A as a matrix that populates the quincunx sub-lattice in 2D, the decomposition formula is

$$\begin{cases} c_{\vec{k}}^{j-1} = \sum_{\vec{n}} \overline{h_{\vec{n}-A\vec{k}}} c_{\vec{n}}^{j}; \\ d_{\vec{k}}^{j-1} = \sum_{\vec{n}} \overline{g_{\vec{n}-A\vec{k}}} c_{\vec{n}}^{j}. \end{cases}$$

In practice, we do the following to obtain c^{j-1} from c^j, note that the the wavelet filters are all in 2D:

Step 1. Convolute c^j with Lo_D;

Step 2. Downsample(quincunx) the result from last step, note that the result is sparse.

Step 3. Rotate the sparse result 45°, to form a dense image, this result is c^{j-1}.

We can repeat the above mentioned process as many times as we want to obtain the desired approximation c^0 and the detail sequences d^0, d^1, ..., d^{j-1}.

In the following example, the input image is decomposed 4 times, resulting $cA4$ and the details sequence $cD4$, $cD3$, $cD2$ and $cD1$.

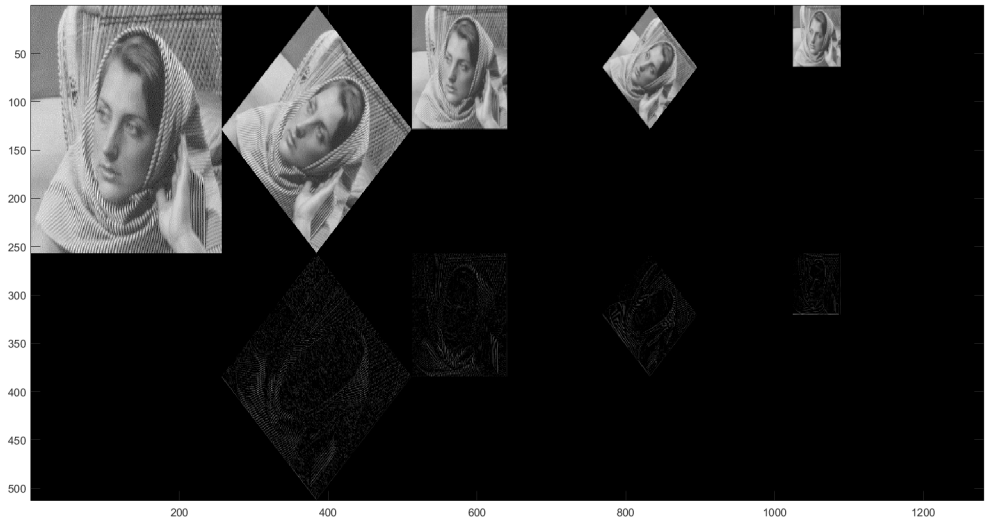

Figure 32: 4-level Image Decomposition

REFERENCES

[1] Benedetto, J and Li, S. The theory of multiresolution analysis frames and applications to filter banks. *Appl. Comput. Harmon. Anal.*, 5(4):389–427, 1998.

[2] X. Dai. Equations For Frame Wavelets In $L^2(\mathbb{R}^2)$. *to appear*, 2015.

[3] X. Dai. Equations For Parseval's Frame Wavelets in $L^2(\mathbb{R}^d)$ with Compact Supports. *preprint*, 2016.

[4] E. Belogay and Y. Wang. Arbitrarily Smooth Orthogonal Nonseparable Wavelets in $\mathbb{R}^2$. *SIAM J. Math. Anal.*, 30(3):678–697, 1999.

[5] A. Haar. Zur Theorie der orthogonalen Funktionensysteme. *Mathematische Annalen*, 69(3):331–371, 1910.

[6] I. Daubechies. Ten lectures on wavelets. *CBMS 61, SIAM*, 1992.

[7] L. Baggett, H. Medina and K. Merrill. Generalized multi-resolution analyses and a construction procedure for all wavelet sets in $\mathbb{R}^n$. *J. Fourier Anal. Appl.*, 5(6):563–573, 1999.

[8] L. Prasad and S.S. Iyengar. Wavelet Analysis with Applications to Image Processing. *CRC Press LLC*, 1997.

[9] S. Mallat. A theory for multiresolution signal decomposition: the wavelet representation. *IEEE Pattern Anal. and Machine Intell.*, 11(7):674–693, 1989.

[10] Y. Meyer. Ondelettes et operateurs(English translation: Wavelets and operators. *Cambridge Univ. Press*, 1993.

[11] Q. Gu and D. Han. On Multiresolution Analysis (MRA) wavelets in $\mathbb{R}^n$. *J. Fourier Anal. Appl.*, 6:437–447, 2000.

[12] W. Huang and X. Dai. Canonical Haar Wavelets in $L^2(\mathbb{R}^2)$. 2016.

[13] W. Lawton. Tight frames of compactly supported affine wavelets. *J. Math. Phys.*, pages 1898–1901, 1990.

APPENDIX A: Some Wavelet Coefficients from Daubechies in [6]

size	n	h_n
N = 2	1	0.7071067811865476
	2	0.7071067811865476
N = 4	1	0.4829629131445341
	2	0.8365163037378077
	3	0.2241438680420134
	4	-0.1294095225512603
N = 8	1	0.2303778133088964
	2	0.7148465705529154
	3	0.6308807679298587
	4	-0.0279837694168599
	5	-0.1870348118790931
	6	0.0308413818355607
	7	0.0328830116668852
	8	-0.0105974017850690

size	n	h_n
N= 16	1	0.0544158422431072
	2	0.3128715909143166
	3	0.6756307362973195
	4	0.5853546836542159
	5	-0.0158291052563823
	6	-0.2840155429615824
	7	0.0004724845739124
	8	0.1287474266204893
	9	-0.0173693010018090
	10	-0.0440882539307971
	11	0.0139810279174001
	12	0.0087460940474065
	13	-0.0048703529934520
	14	-0.0003917403733770
	15	0.0006754494064506
	16	-0.0001174767841248

Table 15: Wavelet Coefficients from Daubechies in [6]

APPENDIX B: Parametric Form Solution for a Lawton's System of Equations

We here will present a parametric form solution for a simple Lawton's System of Equations.

Consider the 1D Lawton's System of Equations with only 4 non-zero terms:

$$\begin{cases} \sum_{n=1}^{4} h_n & = & \sqrt{2}, \\ \sum_{n=1}^{4} h_n^2 & = & 1, \\ h_1 \cdot h_2 + h_3 \cdot h_4 & = & 0. \end{cases} \tag{35}$$

We have a solution in parametric form:

$$\begin{cases} h_1 = \frac{\sqrt{2}}{2} \cdot \frac{t(1+t)}{1+t^2}, \\ h_2 = \frac{\sqrt{2}}{2} \cdot \frac{1+t}{1+t^2}, \\ h_3 = \frac{\sqrt{2}}{2} \cdot \frac{1-t}{1+t^2}, \\ h_4 = \frac{\sqrt{2}}{2} \cdot \frac{-t(1-t)}{1+t^2}, \end{cases} \tag{36}$$

where $t \in \mathbb{R}$.

In particular, we have db4 when $t = \frac{\sqrt{3}}{3}$.

Also, following the process presented in Chapter 3, we can "upgrade" this 1D wavelet coefficients set to a 2D one:

$h_{1,1}$	$h_{2,1}$	h_1	0
$h_{1,2}$	$h_{2,2}$	h_2	h_3
$h_{1,3}$	$h_{2,3}$	0	h_4
$h_{1,4}$	$h_{2,4}$	0	0

Table 16: A Parametric Solution in 2D

The associated matrix populates the quincunx sub-lattice, so $\begin{bmatrix} 1 & 1 \\ 1 & -1 \end{bmatrix}$ fit the bill. This 2D solution is used in Secion 4.2.

APPENDIX C: Matlab Scripts for Secion 4.2

Note that quincunxdown is a customized function that downsamples the input by quincunx sublattice.

```
load woman;
% X contains the loaded image. map contains the loaded colormap.

% for this t's value, we are using 2D version of db4, but other values also work
t = 1/sqrt(3);
H = [t*(1+t),   1+t,    0,         0;
           0,   1-t,    -t*(1-t),  0 ]/(1+t^2)/sqrt(2);

% Decomposition Level 1
% cA
% convolute with low-pass decomp filter
cA1_same = conv2(X,Lo_D,'same');
% downsample by quincunx sublattice, retain even-index sum terms,
% then rotate clockwise to form center dense, diamond shape
cA1 = quincunxdown(cA1_same,0,1);
% cD
% convolute with high-pass decomp filter
cD1_same = conv2(X,Hi_D,'same');
```

```
% downsample by quincunx sublattice, retain even-index sum terms,
% then rotate clockwise to form center dense, diamond shape
cD1 = quincunxdown(cD1_same,0,1);



% Decomposition Level 2
% cA
% use the dense diamond to convolute with low-pass decomp filter
cA2_same = conv2(cA1,Lo_D,'same');
% downsample by quincunx sublattice, retain even-index sum terms,
% then rotate counter-clockwise to form center dense square shape
cA2 = quincunxdown(cA2_same,0,-1);
% cD
% use the dense diamond to convolute with high-pass decomp filter
cD2_same = conv2(cA1,Hi_D,'same');
% downsample by quincunx sublattice, retain even-index sum terms,
% then rotate counter-clockwise to form center dense square shape
cD2 = quincunxdown(cD2_same,0,-1);
cA2_temp = cA2;
% keep only the center non-zero part
cA2 = wkeep(cA2, floor((size(X))/2));
cD2 = wkeep(cD2, floor((size(X))/2));
```

```
% Decomposition Level 3

% cA

cA3_same = conv2(cA2,Lo_D,'same');

cA3 = quincunxdown(cA3_same,0,1);

% cD

cD3_same = conv2(cA2,Hi_D,'same');

cD3 = quincunxdown(cD3_same,0,1);


% Decomposition Level 4

% cA

cA4_same = conv2(cA3,Lo_D,'same');

cA4 = quincunxdown(cA4_same,0,-1);

% cD

cD4_same = conv2(cA3,Hi_D,'same');

cD4 = quincunxdown(cD4_same,0,-1);


% keep only the center non-zero part

cA4 = wkeep(cA4, floor((size(cA2))/2));

cD4 = wkeep(cD4, floor((size(cA2))/2));


% so we have cA4 and the details sequence cD4, cD3, cD2, cD1
```